


RESEARCH

Open Access



Fecal microbiota transfer between young and aged mice reverses hallmarks of the aging gut, eye, and brain

Aimée Parker^{1*} , Stefano Romano¹, Rebecca Ansoorge¹, Asmaa Aboelnour², Gwenaëlle Le Gall³, George M. Savva¹, Matthew G. Pontifex³, Andrea Telatin¹, David Baker¹, Emily Jones¹, David Vauzour³, Steven Rudder¹, L. Ashley Blackshaw¹, Glen Jeffery² and Simon R. Carding^{1,3*}

Abstract

Background: Altered intestinal microbiota composition in later life is associated with inflammaging, declining tissue function, and increased susceptibility to age-associated chronic diseases, including neurodegenerative dementias. Here, we tested the hypothesis that manipulating the intestinal microbiota influences the development of major comorbidities associated with aging and, in particular, inflammation affecting the brain and retina.

Methods: Using fecal microbiota transplantation, we exchanged the intestinal microbiota of young (3 months), old (18 months), and aged (24 months) mice. Whole metagenomic shotgun sequencing and metabolomics were used to develop a custom analysis workflow, to analyze the changes in gut microbiota composition and metabolic potential. Effects of age and microbiota transfer on the gut barrier, retina, and brain were assessed using protein assays, immunohistology, and behavioral testing.

Results: We show that microbiota composition profiles and key species enriched in young or aged mice are successfully transferred by FMT between young and aged mice and that FMT modulates resulting metabolic pathway profiles. The transfer of aged donor microbiota into young mice accelerates age-associated central nervous system (CNS) inflammation, retinal inflammation, and cytokine signaling and promotes loss of key functional protein in the eye, effects which are coincident with increased intestinal barrier permeability. Conversely, these detrimental effects can be reversed by the transfer of young donor microbiota.

Conclusions: These findings demonstrate that the aging gut microbiota drives detrimental changes in the gut–brain and gut–retina axes suggesting that microbial modulation may be of therapeutic benefit in preventing inflammation-related tissue decline in later life.

Keywords: Aging, Microbiota, Gut–brain axis, Gut–retina, Intestine, Fecal microbiota transplantation, Leaky gut, Inflammaging

*Correspondence: aimee.parker@quadram.ac.uk; simon.carding@quadram.ac.uk

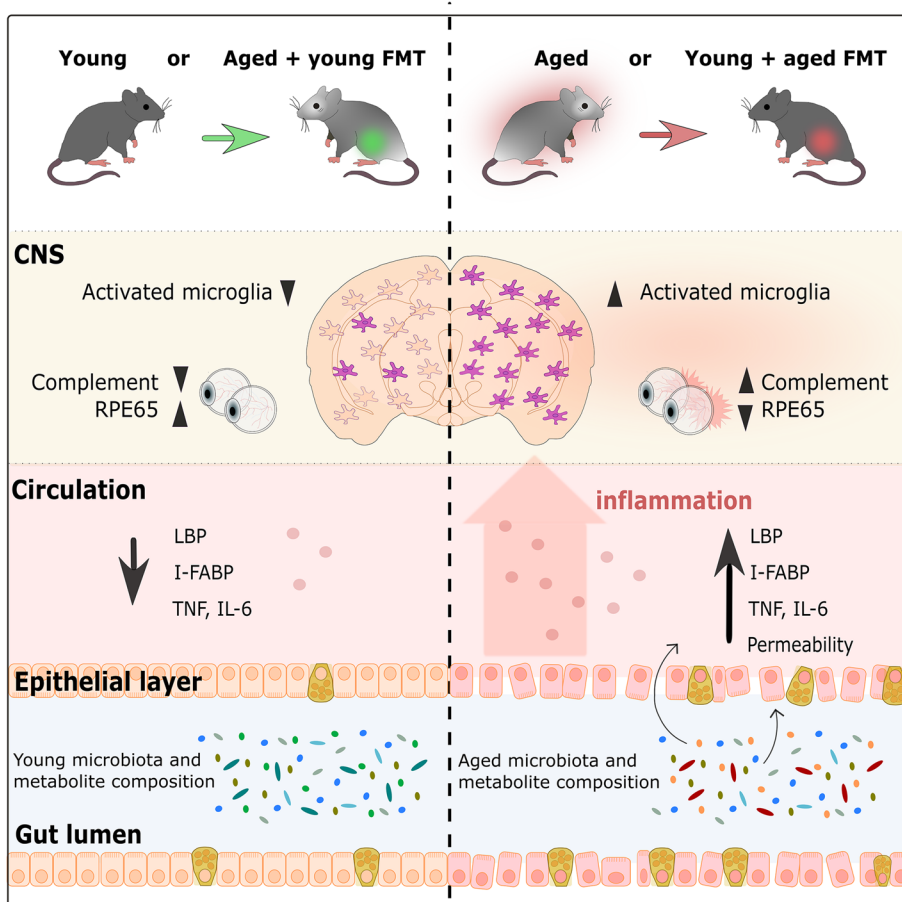
¹ Gut Microbes and Health Research Programme, Quadram Institute, Norwich NR4 7UQ, UK

³ Norwich Medical School, University of East Anglia, Norwich NR4 7TJ, UK

Full list of author information is available at the end of the article



Graphical abstract



Background

Aging is characterized by declining cell, tissue, and organ function and increasing susceptibility to chronic and debilitating diseases. Particularly vulnerable are tissues of the central nervous system (CNS) and the eye, which have high sensitivity to metabolic dysregulation, and the gastrointestinal (GI) epithelial barrier, which must maintain rapid cellular turnover and barrier integrity while faced with constant exposure to environmental insults [14, 85].

Comprising bacteria, viruses, fungi, protozoa, and archaea, the intestinal microbiota contributes to the life-long health of the host, playing key roles in the development and maintenance of the host immune system and the intestinal epithelial barrier [111]. During aging, the intestinal microbiota undergoes changes in the community structure and function, with samples from elderly individuals showing changes in the proportions of different taxa, increased inter-individual variability, and

altered diversity. These changes can adversely affect the host metabolism and immunity [25–27, 40, 64, 86, 110, 112, 118] and are associated with the development of cardiovascular, autoimmune, metabolic, and neurodegenerative disorders [17, 90, 122, 132].

Microbiota transfer studies in fly and fish models of aging suggest a direct role of the microbiota in regulating lifespan and age-associated disease pathogenesis. Young flies fed homogenates from aged flies had significantly decreased lifespan and increased incidence of intestinal barrier dysfunction, compared with flies fed homogenates from young animals [27]. In the short-lived African killifish, the transfer of young donor microbiota to aged individuals ameliorated behavioral decline and extended lifespan [110]. Similar beneficial effects have been reported in aged mice receiving microbiota from young mice to extend life span [8, 61] or halt the functional decline in the mucosal immune system [112].

One of the major organ systems adversely affected by aging and inflammaging is the brain, with various lines of investigation providing evidence for a “microbiota–gut–brain axis” via which gut microbes can influence brain health via various mechanisms. These include complex and interlinked hormonal signaling, immune signaling, and neural signaling networks in the host, which can be modulated by gut microbial products and which can in turn modify the gut microbiota composition and function [90]. Sequencing studies showing associations between particular gut microbiota profiles and various diseases in humans, along with studies modifying the gut bacterial composition in animal models, by probiotic administration or microbiota transfer, implicate the gut microbiota as a key regulator of systemic homeostasis, including neuroinflammation and behavioral disorders [16, 106]. One possible scenario is that changes in the gut microbiota composition or function trigger or, contribute to, the decline of normal gut epithelial barrier function, which in turn drives systemic chronic inflammation that has detrimental effects on various tissues around the body. In aging, detrimental changes in the diversity, composition, or function of the gut microbiota could therefore promote neuroinflammation and functional decline in the CNS.

In the aged GI tract, compromised epithelial and mucosal cell turnover, integrity, and function [32, 36, 76, 83] can lead to increased epithelial barrier permeability [19, 75, 118, 120], with the increased possibility of luminal microbial and dietary antigens gaining access to the circulation. This, together with declining immune cell function and immunosenescence, promotes a state of elevated systemic inflammation termed “inflammaging” [39, 40, 118], contributing to the functional decline in the intestine and CNS in old age [10, 13, 48].

In the brain, microglial cells play multiple roles in regulating inflammatory responses and neural functioning and are now considered central to the pathology of neurodegenerative diseases [48]. Studies using germ-free mice, antibiotic treatment, and selective microbial colonization suggest that the intestinal microbiota can regulate microglial maturation and function in the enteric and central nervous systems [37, 54]. Attenuation of pathology following microbial modulation, in transgenic mouse models of Alzheimer’s disease [57, 115], also supports a role for the microbiota in inflammaging in the brain.

As an extension of the CNS, the eye is exposed to multiple stressors, including oxidative stress-inducing UV light and age-related immune dysregulation, and is vulnerable to energy insufficiency resulting from altered circulation and metabolism in old age [72]. With advancing age, the outer retina of the eye displays elevated inflammation and widespread deposition of extracellular debris,

including amyloid species [55, 88]. Age-related macular degeneration (AMD) is associated with chronic inflammation [29, 65] and altered fecal microbial metabolite profiles [100]. The altered microbial composition has also been associated with neovascularization and immune cell activation in retinal disease models [4, 50, 99].

To investigate the effects of age-associated microbiota composition on inflammaging and its impact on the gut, brain, and retina, we used young (3 months), old (18 months), and aged (24 months) mice. We compared mice receiving microbiota from a different age group (heterochronic) fecal microbiota transplant (FMT) with mice receiving microbiota from the same age group (coeval FMT). Control animals received antibiotics only (antibiotic treatment controls) or PBS only (gavage/procedural controls). We compared the systemic and tissue-specific biomarkers of inflammation and function in the brain and retina, intestinal epithelial barrier integrity, circulating inflammatory markers, and behavioral impacts. To avoid confounding impacts of vendor influences on the microbiota of different age groups, our study used mice of three different ages from the same colony, which were all bred and maintained in the same environment for their entire lifespan. Importantly, we also accounted for any potential cage grouping or housing effects in our analyses.

We show that FMT from between young and aged mice replaced the recipient microbiota composition with a composition resembling the donor, enriched for particular bacterial species, and altered the metabolic potential of the resulting gut microbial composition. Our results demonstrate that the aging microbiota mediates detrimental changes in microglial activation in the brain, and inflammation and functional protein expression in the eye in parallel with altered intestinal barrier permeability. Detrimental effects were accelerated upon transfer of aged donor microbiota into young mice, but conversely, age-associated inflammatory changes were reversed in aged mice by transfer of young donor microbiota.

Methods

Experimental model details

Mice

All mice were bred and maintained under specific pathogen-free (SPF) conditions at the University of East Anglia (UEA) Disease Modelling Unit Facility, housed in individually ventilated cages with three to five mice per cage. Mice were fed a standard chow diet provided with water *ad libitum* and maintained under a 12-h light:12-h dark cycle. Male C57BL/6J mice aged 3, 18, or 24 months were used in this study and were all bred and housed in the

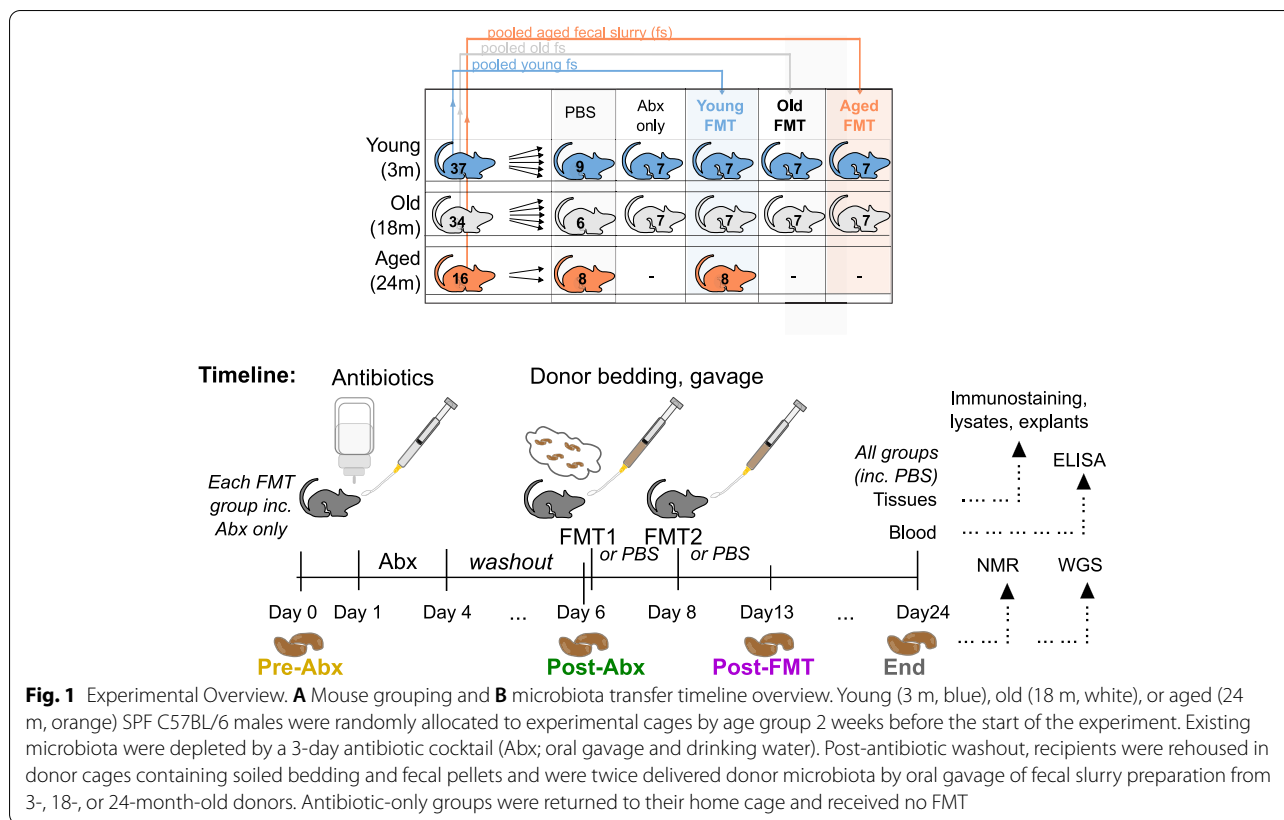


Fig. 1 Experimental Overview. **A** Mouse grouping and **B** microbiota transfer timeline overview. Young (3 m, blue), old (18 m, white), or aged (24 m, orange) SPF C57BL/6 males were randomly allocated to experimental cages by age group 2 weeks before the start of the experiment. Existing microbiota were depleted by a 3-day antibiotic cocktail (Abx; oral gavage and drinking water). Post-antibiotic washout, recipients were rehoused in donor cages containing soiled bedding and fecal pellets and were twice delivered donor microbiota by oral gavage of fecal slurry preparation from 3-, 18-, or 24-month-old donors. Antibiotic-only groups were returned to their home cage and received no FMT

same room. All experiments were approved by the UEA Animal Welfare and Ethical Review Body

Experimental procedures

Microbiota transfer

Groups of young (3 months), old (18 months), or aged (24 months) male mice were randomly re-assigned to experimental cages 2 weeks prior to the start of the experiment. Groups of seven mice (see Fig. 1A), designated for antibiotic/fecal microbiota transfer (FMT) interventions, were sub-housed as groups of three or four due to cage occupancy restrictions. PBS-only groups were also sub-housed in groups of three, four, or five as necessary. Microbiota modulation can be induced by simply co-housing heterochronic groups of mice [112]; however, we chose to also deplete host gut microbiota by prior antibiotic cocktail administration, to maximize potential engraftment of the donor microbiota. Existing microbiota were depleted by delivery of 3-day broad-spectrum antibiotic cocktail regime by combined oral gavage of unpalatable antibiotics (100 µL of vancomycin, 5 mg/mL; metronidazole, 10 mg/mL) while others were able to be provided in drinking water (ampicillin 1 g/L, neomycin 0.5 g/L). Post-antibiotic washout, recipients were rehoused in heterochronic donor cages containing soiled

bedding and fecal pellets and were twice delivered heterochronic donor microbiota 72 h apart by oral gavage of fecal slurry preparation. Pre-Abx samples and FMT slurry are equivalent in that they were prepared from pellets collected at the Pre-Abx time point, with half the sample sent to sequence and half used to prepare the slurry. Fecal slurries were prepared from Pre-Abx donor mice by pooling fecal pellet material from two mice per cage (chosen randomly within each cage), for each age group. Thus, young donor microbiota was a pool representing 20 of 37 mice housed across 10 cages; old donor microbiota was also a pool representing 20 of 34 mice housed across 10 cages. For the aged pool, pellets were included from all 16 mice across four cages. Each mouse received 100 µL fecal slurry preparation at each gavage. At pellet collection, mice were separated into individual sterile boxes and two pellets collected before returning to the cage. The Pre-Abx samples represented in Fig. 5 show the results of sequencing one fecal pellet of the two from each individual mouse. The fecal slurry was produced by combining the second pellets from a random subset of these same mice. The pellets sequenced and represented as the “baseline” composition for each age group in our analyses therefore representing the composition from the mice whose same pellets were delivered as donor pellets

the FMT. Control groups for 3-month-old and 18-month-old mice receiving heterochronic transfer included gavage with PBS only and antibiotic treatment/PBS gavage only, and groups receiving coeval (donor pool of the same age group) soiled cages and gavage. Due to the limited availability of 24-month aged mice, only heterochronic FMT and no-transfer controls were possible for this age group. Transfer of soiled bedding was repeated every 3 days. Fecal pellets were collected for sequencing at “Pre-Abx,” “Post-Abx,” “Post-FMT” (7 days post-transfer), and “end” (18 days post-transfer) time points (see Fig. 1B). Pellets were collected from all mice at the four time points, after briefly separating into single-occupancy sterile boxes, and collected using sterile picks and DNA/RNA-free sterile microtubes, which were then stored at -80°C until DNA extraction. NMR analysis used pellet samples at the “end” time point. Blood and tissues were also collected at the end of the experiment. Fecal pellets, blood, and tissue collections and FMT interventions were all performed at the same time of day across all cages to account for circadian rhythm variability in feeding and microbiota/metabolite composition.

Metagenomic library preparation and sequencing

Genomic DNA from fecal samples was isolated using the FastDNA SPIN Kit for Soil (MP Biomedicals), quantified using the Qubit dsDNA BR Assay Kit and Qubit 3.0 fluorimeter (Invitrogen) and normalized to 5 ng/ μL . A miniaturized reaction was set up using the Illumina Nextera DNA Flex Library Prep Kit (Illumina). 0.5 μL Tagmentation Buffer 1 (TB1) was mixed with 0.5 μL bead-linked transposomes (BLT) and 4.0 μL PCR-grade water in a master mix and 5 μL added to a chilled 96-well plate. Two microliters of normalized DNA (10 ng total) was pipette mixed with the 5 μL of the tagmentation mix and heated to 55°C for 15 min. PCR master mix (Kap2G Robust PCR kit, Merck) was combined with P7 and P5 Nextera XT Index Kit v2 index primers (Illumina) and tagmentation mix and amplified by PCR. Libraries were quantified using the Quant-iT dsDNA Assay high-sensitivity kit (Invitrogen) and run on a GloMax[®] Explorer Multimode Microplate Reader (Promega). Libraries were pooled in equal quantities following quantification. The final pool was double-SPRI size selected between 0.5 and $0.7\times$ bead volumes using KAPA Pure Beads (Roche), quantified on a Qubit 3.0 fluorimeter and run on a D5000 ScreenTape system (Agilent) using the Agilent TapeStation 4200 to calculate the final library pool molarity. “Kitom” controls (water and PBS controls processed through the same DNA extraction process as all samples) were included along with the DNA extraction process, but these control samples then failed at the library preparation step due to very low available input material. This

suggests there was no or insufficient DNA contamination resulting from the kit to be of significance to the subsequent analysis of the metagenomic data. Libraries were sequenced by NGS Illumina sequencing to a depth of 10 Gbp/sample by Novogene, UK. Per-sample read numbers are shown in Supplementary Fig. S6.

Metagenomic sequence data processing

Raw sequence reads were trimmed to a quality of phred 20, and adapters and PhiX Illumina standards removed using BBDuk v38.76 (sourceforge.net/projects/bbmap/) [20]. Human read contamination was removed using BBMap v38.76 and a masked reference of the hg19 dataset released by Brian Bushnell (<https://zenodo.org/record/1208052#.X9DiS6r7SHw>). Reads mapping to the mouse genome (*Mus musculus* GRCm38) were removed using BBMap v38.76 (parameters: *minid=0.95; maxindel=3; bwr=0.16; bw=12; quickmatch; fast; minhits=2*). Taxonomic profiling was performed on the filtered reads using MetaPhlAn (v3.0.0.0-alpha) [12, 107], including estimation of the unknown fraction (parameter: *--unknown_estimation*) with the database mpa_v30_CHOCOPhlAn_201901. Functional read profiling was performed using HUMAnN3 (v3.0.0.alpha.1) [12, 41] including MetaPhlAn, DIAMOND v0.9.24 [18], and the databases uniref90 (v201901) [116] and mpa_v30_CHOCOPhlAn_201901.

Alpha and beta diversity analyses

Species relative abundances obtained from MetaPhlAn (v3.0.0.0-alpha) were imported into R [92] and manipulated using the *phyloseq* package v1.30.0 [79]. The number of observed species was calculated using the *richness* function in the R package *microbiome* v1.8.0 [63]. Statistical differences in the number of observed species across the different groups were tested using linear mixed models (*lmm*) with cage as a random effect (*observed species ~ time point + (1|cage)*). Models were built using the *lmer* function in *lme4* v1.1.21 [9] R packages, and pairwise contrasts were extracted using the *emmeans* v1.4.5 [69] function with default parameters.

Beta-diversity analyses were initially performed using Bray–Curtis (BC) and Jensen–Shannon divergence (JSD) indices on all samples obtained throughout the experiment. Ordinations were built using PCoA, and negative eigenvalues were set to 0. While the BC index allowed better visualization of the data, JSD explained a greater proportion of data variance and thus was used for further testing. To verify the divergence between time points and simultaneously account for cage effect, we used a JSD distance matrix and created a dBRDA, conditioning the data for cage and constraining per time point. dBRDA was performed using the “CAP” option in the *ordinate*

function in *phyloseq*. The resulting model was used to perform a permutational ANOVA, function *anova.cc* in the *vegan* v2.5.6 [89] R package, limiting the permutation within cages (permutations = how (blocks = cage, nperm = 10,000)). Pairwise PERMANOVA [5] were carried out between time points using *pairwiseadonis* v0.0.1, limiting the 10,000 permutations within cages and using Benjamini–Hochberg (BH) for *P* value correction. Additional ordinations were done for samples obtained at the beginning of the experiment (Pre-Abx) and for samples of young mice receiving either young or aged FMT and old mice receiving young FMT (Post-FMT). Ordinations used JSD as indicated above. Pairwise PERMANOVA was used to assess microbiota divergence between groups using BH *P* value correction. For comparison between pre- and post-FMT, permutation was restricted within cages (*strata* = cage). Since recipients were confounded within cages, free permutation was allowed in the pairwise comparisons for the Pre-Abx dataset. To infer species that were major drivers of sample divergence in the beta diversity analyses, species abundance was correlated to the ordinations using the *envfit* function in the R *vegan* package allowing 10,000 permutations. *P* values were corrected using false discovery rate (fdr), and only taxa showing $P < .005$ and the strongest degree of variation along the axis ($\geq |0.43|$) were selected. All species showing $P < .05$ were instead plotted on the ordination including only samples referring to the Pre-Abx time point. Finally, *procrustes* tests were used to estimate the correlation between ordinations obtained for single time points. PCoA ordinations obtained for the shared samples across time points were used to run a *protest* in the R *vegan* package allowing 10,000 permutations.

Differential abundance analyses

Differential abundance (DA) analyses were performed using linear mixed models (*lmm*) for family and species, and the unstratified pathways were obtained from MetaPhlAn (v3.0.0.0–alpha). For taxonomy, *lmm* were built using samples from Pre-Abx, Post-FMT, and at the end of the experiment. To accommodate the different data distributions of each species, we built *lmm* and tested multiple transformations, building *lmm* for each, using centered log ratios (function *codaSeq.clr* in the R package *CodaSeq* v0.99.6) [44], log₂, ArcSin, and logit, all performed after adding a constant to 0 values, and log₂Zero, where Na/Inf, derived from the log transformation, were converted to 0. Residuals were manually inspected. We selected all *lmm*-transformation combinations that had roughly random and normally distributed residuals. We then selected all species that had significant *P*-values for each contrast of interest (e.g., Pre-Abx vs. Post-FMT).

Finally, to homogenize the results, we reported the CLR transformed data for the final figures as presented. For the metabolic pathway analysis, we again tested multiple transformations, and *lmm* were also built on non-transformed data as this condition produced residuals roughly randomly and normally distributed. Differential abundance analysis was performed after filtering the datasets retaining all species with relative abundance > 0 in $\geq 5\%$ of samples and all genera and families with relative abundance > 0 in $\geq 15\%$ of samples. Only pathways present in all samples of at least one time point across the groups were considered (e.g., all samples of young receiving old FMT at the beginning of the experiment). *lmm* were built as follows: $taxa/path \sim receiver * donor * time\ point + (1|cage/mice)$. Specific contrasts were selected using the *emmeans* function ($specs = \sim receiver:donor:time\ point$) without *P* value correction. After obtaining all contrasts of interest for all taxa/pathways, all *P* values were corrected using fdr. Finally, to test the differential abundance of species Pre-Abx between the age groups, we selected only the samples relative to this time point and built the *lmm*: $taxa/path \sim receiver + (1|cage)$ using the approach specified above and considering only species with a relative abundance > 0 in $\geq 10\%$ of samples. The extraction of the contrasts and *P* value correction were performed as above.

Analysis of fecal metabolite concentrations by nuclear magnetic resonance (NMR)

Fecal samples were homogenized in 1:12 w/v of saline phosphate buffer (1.9 mM Na₂HPO₄, 8.1 mM NaH₂PO₄, 150 mM NaCl) with 1 mM sodium 3-trimethylsilyl-propionate-d₄ (TSP-d₄) mixed 1:1 v/v with deuterated water (Merck) using ceramic bead beating (Lysing Matrix E, MP Biomedicals), followed by centrifugation at 15,000g, 5 min, and filtration of supernatants at 0.2 μm. ¹H NMR spectra were recorded using a 600-MHz Bruker Avance spectrometer fitted with a 5-mm TCI proton-optimized triple resonance NMR inverse cryoprobe and autosampler (Bruker). Sample temperature was controlled at 300 K. Spectra were transformed with a 0.3-Hz line broadening and zero filling, manually phased, baseline corrected, and referenced by setting the TSP-d₄ signal to 0 ppm. Metabolites were identified by comparison with existing literature, an in-house database of mouse fecal metabolite spectra, the Human Metabolome Database (<http://www.hmdb.ca/>), and by use of 2-dimensional NMR ¹H–¹H correlation spectroscopy, ¹H–¹³C heteronuclear single quantum correlation, and ¹H–¹³C heteronuclear multiple bond correlation spectroscopy [67, 68, 121]. Concentrations were calculated using Chenomx NMR Suite 7.0, centered (CLR), and log-transformed.

Metabolome data analysis

Only metabolites present in > 10% of samples or at least three individual animals within one experimental group were analyzed. Data were log₂-transformed after adding a constant (0.001) to 0 values and were centered using the function *scale* in R. After calculating, the Euclidean distance data were plotted using PCoA. One sample from the aged Pre-Abx group was removed as it clearly represented an outlier in the ordination. A dbRDA model was then built constraining the data for mouse groups and conditioning the data for cage. Permutational ANOVA on the model (*anova.cca*) was then performed restricting the 10,000 permutations within cages. Similarly, pairwise PERMANOVA on the Euclidean distance matrix was performed using 10,000 permutations restricted within cages and correcting *P* values using FDR. Sparse PLS-DA was performed using the function *splsda* in the R package *mixOmics* v6.10.9 [96]. Model performance and component and variable selections were tested using a five-fold validation and 75 repetitions with the functions *perf* and *tune.splsda* within the *mixOmics* package. Differential abundance analysis was initially performed using lmm as specified above on scaled values. Since models showed a poor fit (residuals not randomly or normally distributed), we performed the analysis using a Kruskal–Wallis non-parametric test, blocking the dataset for cages. For this purpose, we used the *kruskal_test* function in the R package *coin* v1.3.1 [51]. *P* values were corrected using FDR.

Quantification of serum/intestinal proteins

Blood samples collected at the end of the experiment were allowed to coagulate for 30 min at room temperature, before centrifugation at 1500g for 10 min. The serums were removed and stored at –80 °C until further use. Serum I-FABP, lipopolysaccharide-binding protein (LBP), and IL-6 were measured using specific ELISAs or as part of a mouse magnetic Luminex panel (detailed in resources file). Lower detection limits of specific ELISAs: I-FABP 0.15 ng/μL, LBP 0.8 ng/mL, IL-6 24.6 pg/mL, and TNF 0.29 pg/mL. Intestinal lysates were prepared from duodenal samples. Tissue samples (50 mg) were homogenized in CellLytic MT (Merck) with added complete protease inhibitor cocktail (Roche) using a FastPrep Bead Beater and Lysing Matrix D tubes (MP Biomedicals) and centrifuged 15 min at 17,000g, 4 °C. Duodenal lysate tumor necrosis factor (TNF) was measured using specific ELISA (detailed in key resources). Total protein concentrations in the serum and lysates were normalized by Bradford assay (BCA protein assay) prior to use in ELISA/Luminex. Four-parameter logistic regression fits for a 6-point standard curve, interpolation of sample concentrations (triplicate serum samples from *n* = 5 mice per group).

Quantification of retinal proteins

Levels of ~40 target cytokines were assayed using a Proteome Profiler Mouse Cytokine Array (BioTechne), using retinal lysates from aged mice young donor microbiota vs. aged donor microbiota (*n* = 8 mice/group). Lysates were generated for whole individual retinæ by lysis in PBS + complete protease inhibitors (SigmaFast), sonication to disrupt cell membranes, freeze-thaw with detergent (Triton X-100), and clarification by centrifugation (10 min at 17,000g, 4 °C, before storage at –80 °C. Pooled lysates (*n* = 8 retinæ/group) were incubated with antibody panel-coated membranes overnight at 4 °C, and the rest of the procedure was performed as per the manufacturer's instructions. Chemiluminescent detection of membranes used a ChemiDoc XRS system (BioRad), and images were exported to dedicated analysis software (ImageLab, BioTechne) for quantification. Following background removal and control membrane (PBS, no lysate) removal, pixel intensities were converted to % change in aged + young FMT vs. aged + aged FMT membranes for each target spot. Nine targets which fell below the threshold of detection or below the control membrane intensity are not displayed.

Retinal immunostaining and quantification

Eyes were fixed 20 min in 4% paraformaldehyde (PFA) before cryopreservation and embedding in OCT compound (Agar Scientific). Cryosections were prepared at 5 μm and stained with goat polyclonal antiserum against complement C3 (MP Biomedicals) or mouse monoclonal antibody to RPE65 (Merck Millipore) and secondary antibodies donkey anti-goat A488, donkey anti-mouse A568 (Invitrogen) nuclei stained with DAPI (Merck). Images were collected using an epifluorescence widefield microscope. The average pixel intensity of a 1280-μm area of the interface between the RPE and Bruch's membrane interface was measured in Adobe Photoshop CS5. Five mice (retinæ) were analyzed per age per group.

Brain Iba-1 cell staining and counts

Brains were formalin-fixed, paraffin-embedded, and sagittal sections were prepared at 4 μm. Iba1-positive microglia were detected by immunostaining with rabbit monoclonal antibody against Iba-1 (1:200, Abcam), donkey anti-rabbit Alexa-594 secondary antibody (Invitrogen), and Hoechst as the nuclear stain. Images were captured by Zeiss LSM880 confocal microscope and the Zen 2010 software. The choice of the cortex and corpus callosum for the analysis was based primarily on our initial observations that Iba-1 densities appeared different between pre- and post-treatment groups in these areas. Cell counts were performed in FIJI/ImageJ [101, 105]. Using images of the Iba-1 channel (A594) only,

background random pixel noise was reduced using the “Despeckle” function. The threshold was then set the same for all images and images made binary. Triplicate area-matched circular regions of interest (ROIs) were placed to encompass as much of the tissue section as possible. The ROIs were then re-used for all images so that identically sized areas were captured for each image. The “Analyze Particles” function was then used to count particles within the three regions, and the results were exported to Excel. Three regions of interest per image, per section, per mouse, and per brain region were analyzed, $n = 5-7$ mice per group. Where any groups have fewer than 7 points represented in Fig. 2, this reflects the exclusion of any samples which had gaps/folds or auto-fluorescent debris within one or more ROIs.

Behavioral tests

To assess the impact of FMT upon cognition and behavior, Y-maze spontaneous alternation test and novel object recognition (NOR) were performed as previously described [91]. Aged mice were tested pre- and post-FMT with young donor fecal microbiota ($n = 10$) and compared with aged control mice receiving aged donor microbiota ($n = 10$), and with young baseline mice ($n = 11$). Briefly, mice were placed into the Y-maze and allowed to explore freely for 5 min while tracking software recorded zone transitioning and locomotor activity (Smart 3.0 tracking software, Panlab, Kent, UK). Spontaneous alternation was calculated using the following formula: spontaneous alternation = (number of alternations/total arm entries - 2) \times 100. Novel object recognition (NOR) was conducted as follows: on day 1, mice were habituated to the empty maze, being allowed to move freely for 10 min. On day 2, mice were conditioned to a single object for a 10-min period. On day 3, mice were placed into the same experimental area in the presence of two identical objects for 15 min, after which they were returned to their respective cages and an inter-trial interval of 1 h was observed. One familiar object was replaced with a novel object. Mice were placed back within the testing area for a final 10 min. Videos were analyzed for a 5-min period, after which if total object exploration time failed to reach an accumulative 10 s, the analysis continued until the 10 s was met. Animals not achieving 10 s were excluded from the analysis. Similarly,

animals not achieving a cumulative 10 s with the familiar object were excluded. The discrimination index was calculated as follows: $DI = (TN - TF)/(TN + TF)$, where TN is the time spent exploring the novel object and TF is the time spent exploring the familiar object.

Statistical analysis

Statistical analysis of microbial diversity and pathway differential abundance were performed as described in detail above in the “Alpha and beta diversity analyses,” “Metabolome data analysis,” and “Differential abundance analyses” sections. Other standard statistical tests (as stated in figure legends) were performed in *Jamovi*, v1.1.9.0 [117] using P values $< .05$ as the cutoff for significance. Typically, pairwise group comparisons were made within age groups between PBS-only and FMT-treated mice and for PBS-only mice between the age groups.

Results

Using FMT, we exchanged the fecal microbiota of the “young” (3-month-old), “old” (18-month-old), and “aged” (24-month-old) groups of C57BL/6 mice (referred to throughout as “young,” “old,” and “aged” mice, respectively). The experimental design and timeline are summarized in Fig. 1. Tissues and blood were collected at the end of the experiment (Fig. 1, “end”) to determine the impact of heterochronic FMT on the susceptibility of key tissues and organs to inflammaging, in particular, the brain, retina, and intestinal epithelium.

The intestinal microbiota regulates microglial activation in the CNS

Using immunohistochemistry, we quantified activated microglial cells, a hallmark of inflammatory neuropathology [48], using the marker Iba-1, in both “gray” and “white” matter areas (cortex and corpus callosum), in the sagittal brain sections of all groups of mice following FMT (Fig. 2 and Fig. S1). Iba-1⁺ microglial cell densities were higher in both the cortex and corpus callosum in old and aged mice compared with young mice (Fig. 2 and Fig. S1, Welch’s t test PBS groups young vs. aged cortex $P = .005$, corpus callosum $P < .001$). No significant differences were seen between the old (18 months) and aged (24 months) control, PBS-treated groups. In young mice, there were no significant differences in Iba-1⁺ cell counts

(See figure on next page.)

Fig. 2 Inflammatory (Iba-1⁺) microglia density in cortex and corpus callosum is regulated by the intestinal microbiota. **A** Iba-1⁺ microglia were identified by immunostaining (red), nuclei counterstained with Hoechst (blue), and quantified in the cortex and corpus callosum (highlighted in cartoons) of sagittal mouse brain sections from all groups of mice. **B** Quantification of Iba-1⁺ cells in the cortex, average count across 3 regions of interest (ROI) from each of 4–7 mice per group from all groups. **C** Quantification of Iba-1⁺ cells in the corpus callosum, an average of 3 regions of interest from each of 4–7 mice per group from all groups. Statistical analysis between the groups of interest by Welch’s t test; error bars denote 95% CI. Significant values are in bold. **D** Representative immunostaining of Iba-1⁺ cells in the cortex of young, old, and aged mice, either treated with PBS only, treated with antibiotics only, or with antibiotics followed by FMT from young, old, or aged donors (see also Fig. S1)

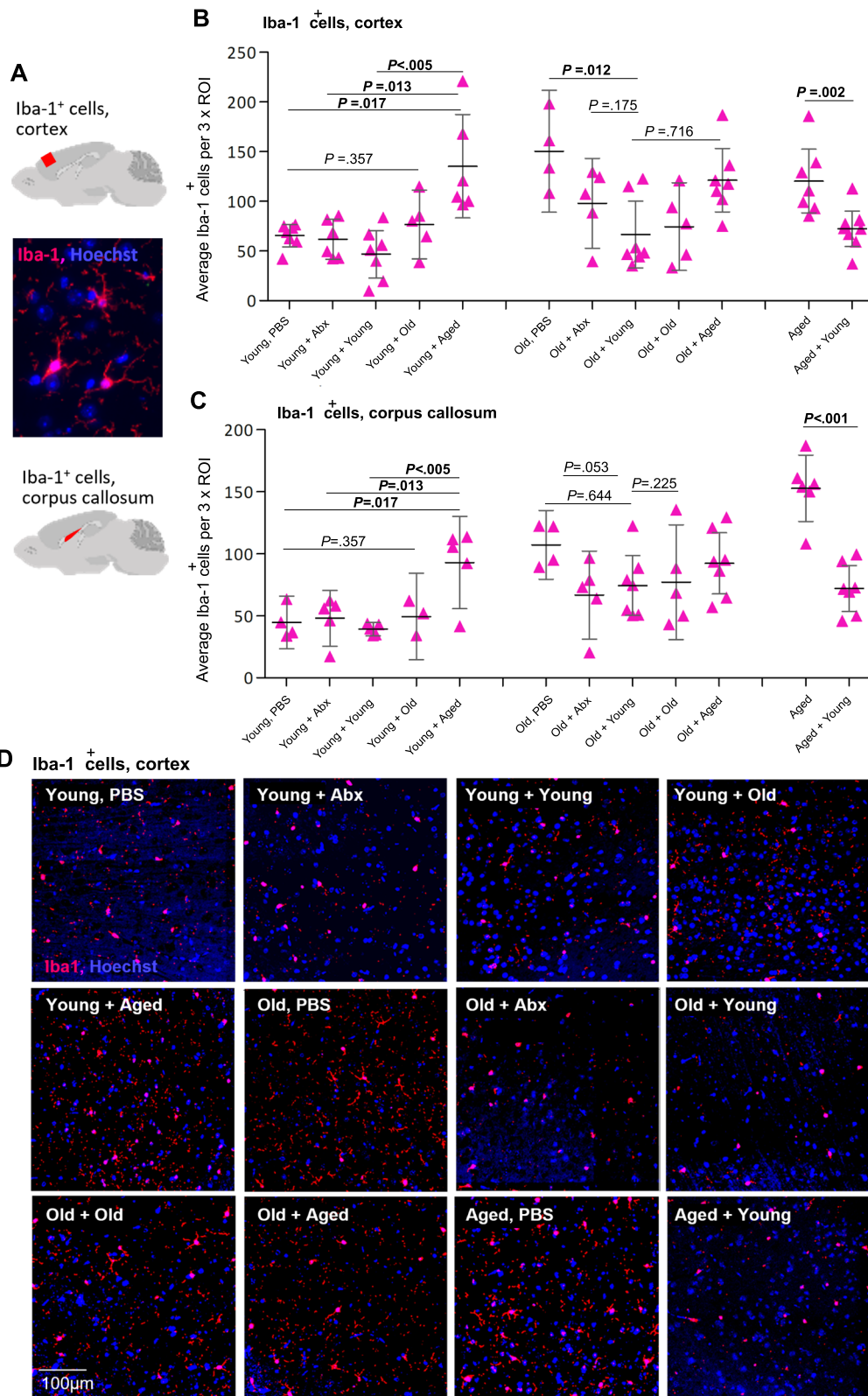


Fig. 2 (See legend on previous page.)

between mice receiving mock transfer, coeval (young) transfer, or old (18 months) donor microbiota. However, young mice that received aged (24 months) donor microbiota had significantly more Iba-1⁺ cells in both the cortex and corpus callosum compared with all other young treatment and control groups that were at levels comparable to those in aged mice (Fig. 2B–D and Fig. S1). Conversely, in aged and old mice receiving young donor microbiota, Iba-1⁺ cells were significantly decreased in the cortex and in the corpus callosum compared with controls (Fig. 2B–D and Fig. S1).

Collectively, these data demonstrate that the intestinal microbiota strongly influences microglia activation and that heterochronic FMT modulates levels of Iba-1⁺ microglia, increasing the levels in young adult mice transplanted with an aged donor microbiota and reducing them in the CNS of aged animals receiving a young donor microbiota.

Chronic inflammation and microglial overactivation in the brain contribute to neurodegenerative pathology, which in turn can lead to cognitive decline [48]). We therefore assessed whether the reversal of inflammatory microglial upregulation in aged mice by FMT may translate to any improvement in established tests of murine cognitive function. We compared aged mice pre- and post-receipt of either a young or aged donor FMT using the Y-maze, a test of spatial working memory, and the novel object recognition (NOR) test, a measure of recognition memory. Although aged mice showed decreased performance in the NOR test at baseline, there was no significant improvement in aged mice receiving a young donor microbiota transfer compared to controls in either test (Supplementary Fig. S5). Our data does not support an impact of short-term microbial modulation by FMT on measures of working spatial and recognition memory in aged mice.

Heterochronic FMT reverses age-associated retinal inflammation

Having identified regulatory effects of heterochronic FMT on inflammation in the CNS, both in the white and gray matter areas of the brain, we next considered the retina, as it is considered an extension or “end organ” of the central nervous system and is also especially vulnerable to age-related functional decline and inflammatory damage. Increasing expression of inflammatory complement protein C3 in the aging rodent retina is associated with progressive extracellular deposits between the retinal pigment epithelium (RPE) and Bruch’s membrane (BM), which contribute to retinal degeneration [7, 103]. Given that our results in the brain showed the most significant impact of heterochronic FMT in the young and aged groups, we characterized the retinal response to FMT

in those age groups. At baseline, aged mice showed significantly more staining for complement C3 at the RPE/BM interface compared with young mice (Fig. 3A and B). Young mice receiving aged donor microbiota showed an increase in retinal complement C3 in this region (Fig. 3A, B) compared with control groups, up to levels comparable to aged mice. In contrast, aged mice receiving young donor microbiota showed a significant reduction in C3 staining compared with PBS-only aged controls, to levels comparable to those in young mice (Fig. 3A, B).

The photoreceptors of the retina are especially sensitive to fluctuations in systemic inflammation and metabolism in old age. Retinal pigment epithelial protein RPE65, which is critical for regeneration of retinal visual pigment in photoreceptors, was depleted in aged mice compared with young mice (Fig. 3C, D). In young mice, baseline levels of RPE65 were reduced post-transfer with an aged donor microbiota (Fig. 3C, D). Strikingly, the transfer of a young donor microbiota into aged mice restored RPE65 expression to levels seen in young mice (Fig. 3C, D). Retinal inflammation and degeneration have been reported to commence earlier than 24 months in rodents [22, 103, 129]. Therefore, along with our young (3 months) and aged (24 months) groups, we also assessed the old (18 months) group and found that although RPE65 staining progressively declined with age (Fig. 3D), C3 staining was not significantly different between the old (18 months) and aged (24 months) PBS groups.

We also assessed the cytokine levels in retinal lysates in aged mice receiving FMT, using a proteome profiling array. Multiple pro-inflammatory cytokines elevated in aged mice were reduced after transplantation of young microbiota including CCL11 (eotaxin), CXCL11, and IL-1 β . On the other hand, IL-13 which is a putative neuroprotective cytokine [98] showed the highest increase following FMT from young donors into aged mice.

Together, our data support a causal role for the gut microbiota–retina axis in regulating retinal inflammation and age-related cytokine signaling, along with the expression of a key functional visual protein (RPE65).

Heterochronic FMT reverses age-associated breakdown of epithelial barrier integrity and systemic inflammation

Inflammaging and pathological inflammation in the CNS have been associated with loss of intestinal epithelial barrier integrity, so-called leaky gut. Here, we investigated whether FMT had any impacts on serum levels of the intestinal epithelial cell protein intestinal fatty acid-binding protein (I-FABP), a key indicator of microbiota-related epithelial cell damage and disruption [66] and a surrogate biomarker of intestinal epithelial permeability [42, 71, 125, 127]. Serum I-FABP concentration was increased by \sim 30% in the

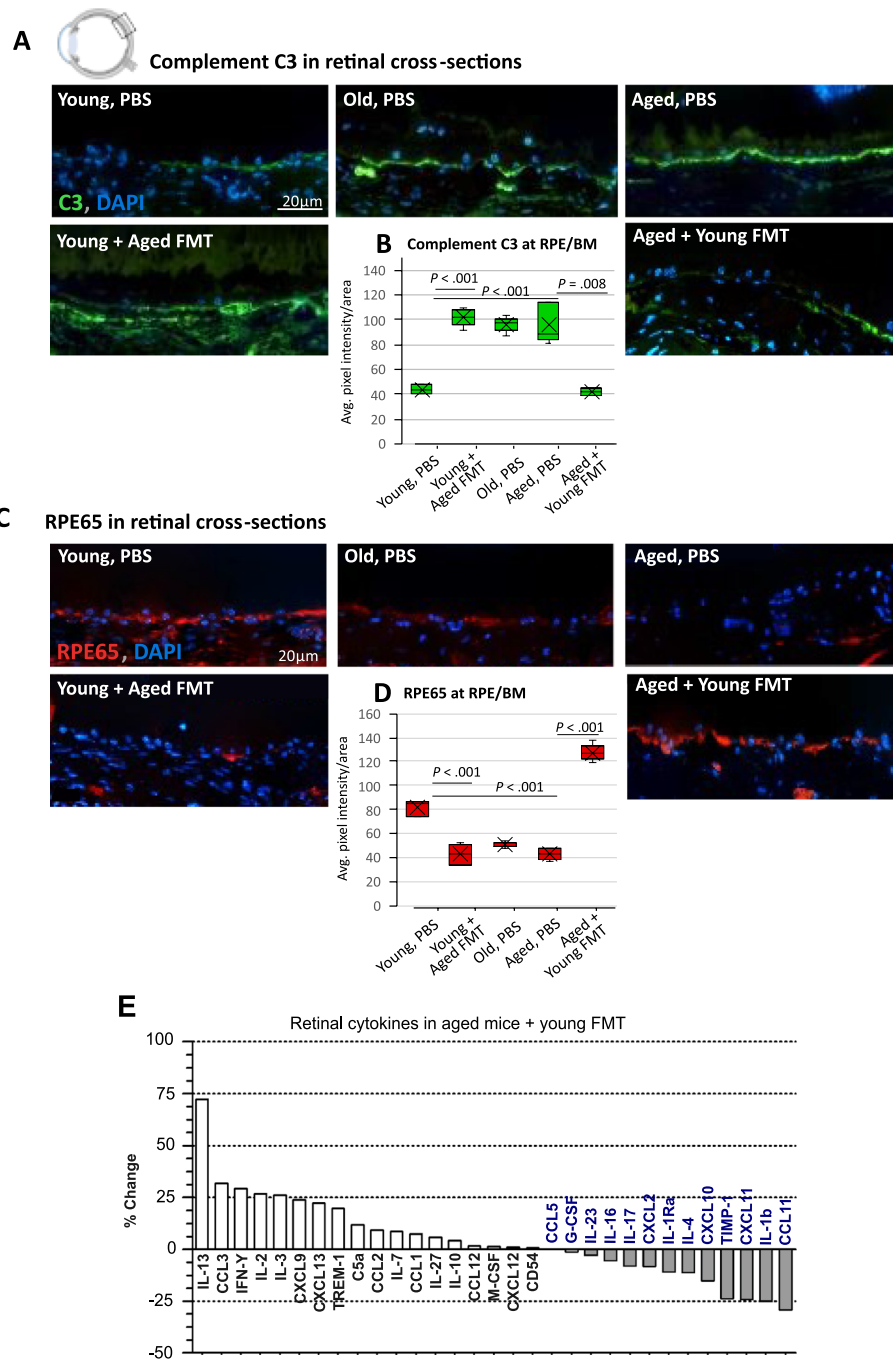


Fig. 3 Heterochronic microbiota transfer reverses age-associated retinal inflammation and functional visual protein expression. **A** Immunostaining of complement C3 (green) in the cross-sections of the retinal pigment epithelium (RPE)/Bruch’s membrane (BM) interface from mice receiving PBS vs. heterochronic FMT. **B** Quantification of the average complement C3 staining pixel intensity (PI) per area (1280 µm²) at the RPE/BM interface in young, old, or aged PBS-treated mice vs. heterochronic FMT (*n* = 5 mice/group). **C** Immunostaining (RPE65, red; nuclei DAPI, blue) and quantification (**D**) of the crucial visual cycle protein RPE65 in the cross-sections of the RPE/BM interface from untreated mice vs. mice receiving heterochronic FMT, *n* = 5 mice/group. Statistical comparison between ages and between the FMT and PBS groups by Welch’s *t* test. **E** Percentage change in the expression of retinal lysate cytokine levels in aged mice receiving young donor FMT

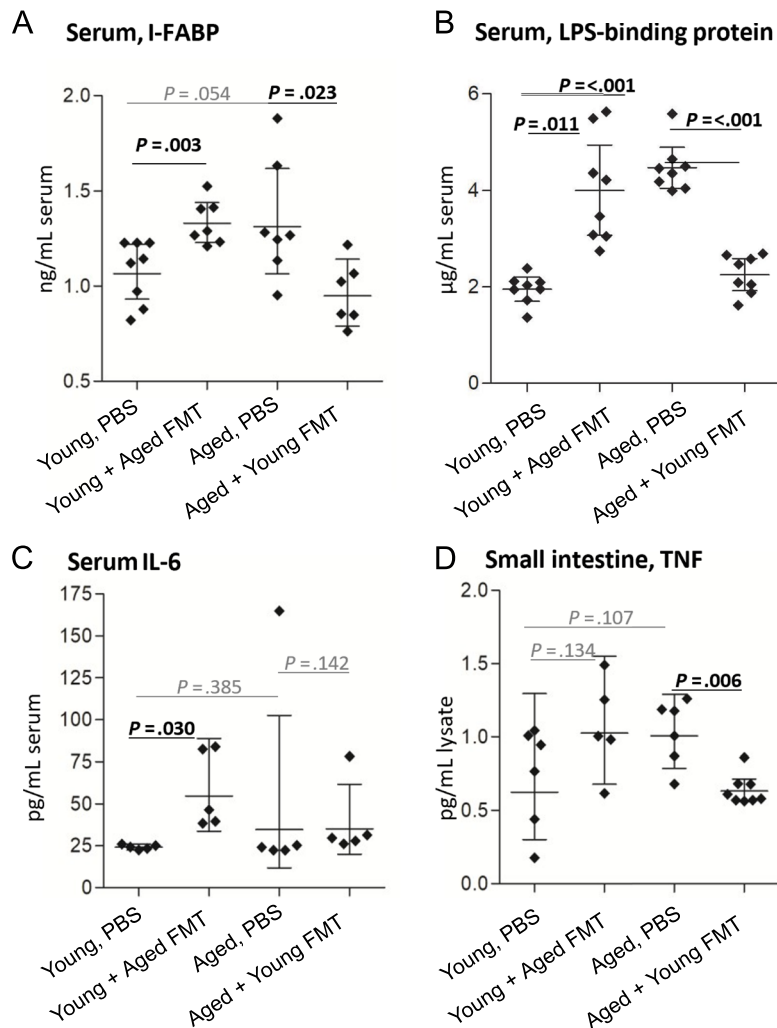


Fig. 4 Heterochronic FMT reverses age-associated breakdown of epithelial barrier integrity and systemic inflammation. **A** ELISA analysis of serum intestinal fatty acid-binding protein (I-FABP) in young and aged mice ($n = 6\text{--}8/\text{group}$) before and after heterochronic FMT. **B** ELISA analysis of serum lipopolysaccharide-binding protein ($n = 8/\text{group}$). **C** Serum levels of IL-6 were analyzed by multiplex magnetic bead assay (Luminex) ($n = 5/\text{group}$). **D** TNF levels in small intestinal tissue lysates as measured by specific ELISA ($n = 5\text{--}8/\text{group}$). Statistical comparison between ages and between FMT and PBS groups by Welch's *t* test; error bars denote 95% CI; significant results in bold black text

young mice receiving aged donor microbiota compared with young mice receiving PBS and conversely was reduced by $\sim 30\%$ in aged mice receiving young donor microbiota compared with aged mice receiving PBS (Fig. 4A). Serum concentrations of lipopolysaccharide (LPS)-binding protein (LBP), which is secreted by the liver in response to bacterial LPS leakage into the bloodstream (and which accelerates inflammaging [56], were approximately two times higher in aged mice than in young mice (Fig. 4B) and were increased in young mice receiving an aged donor microbiota, to levels comparable to aged mice. Conversely, aged mice receiving young donor microbiota had reduced

circulating concentrations of LBP, to levels comparable to young mice. Analysis of the key inflammaging-associated cytokines, IL-6 and tumor necrosis factor (TNF) [95], showed elevated concentrations of serum IL-6 in young mice receiving an aged donor microbiota, approximately twice as high as in young mice receiving PBS (Fig. 4C), with no significant difference seen between any other groups. Levels of TNF were reduced by around 40% in small intestinal lysates from aged mice receiving young donor microbiota, while pre- and post-transplant levels were not significantly different in young mice receiving an aged donor microbiota (Fig. 4D). Our cytokine analysis also included IL-12,

IL-17, IL-1 β , and IL-27, but none of these was above the assay threshold of detection in any group (data not shown).

Together, these data demonstrate that the aged microbiota promotes the breakdown of epithelial barrier integrity, the translocation of bacterial products, and the elevated serum levels of pro-inflammatory cytokines, all of which were reversed by transplantation with young donor microbiota.

Next, we investigated how the microbiota changes with age and following FMT, with the aim of identifying microbial signatures and features that could account for inflammaging and the beneficial outcomes of young donor FMT in aged recipients.

Donor-derived species define the intestinal microbiota composition of FMT recipients

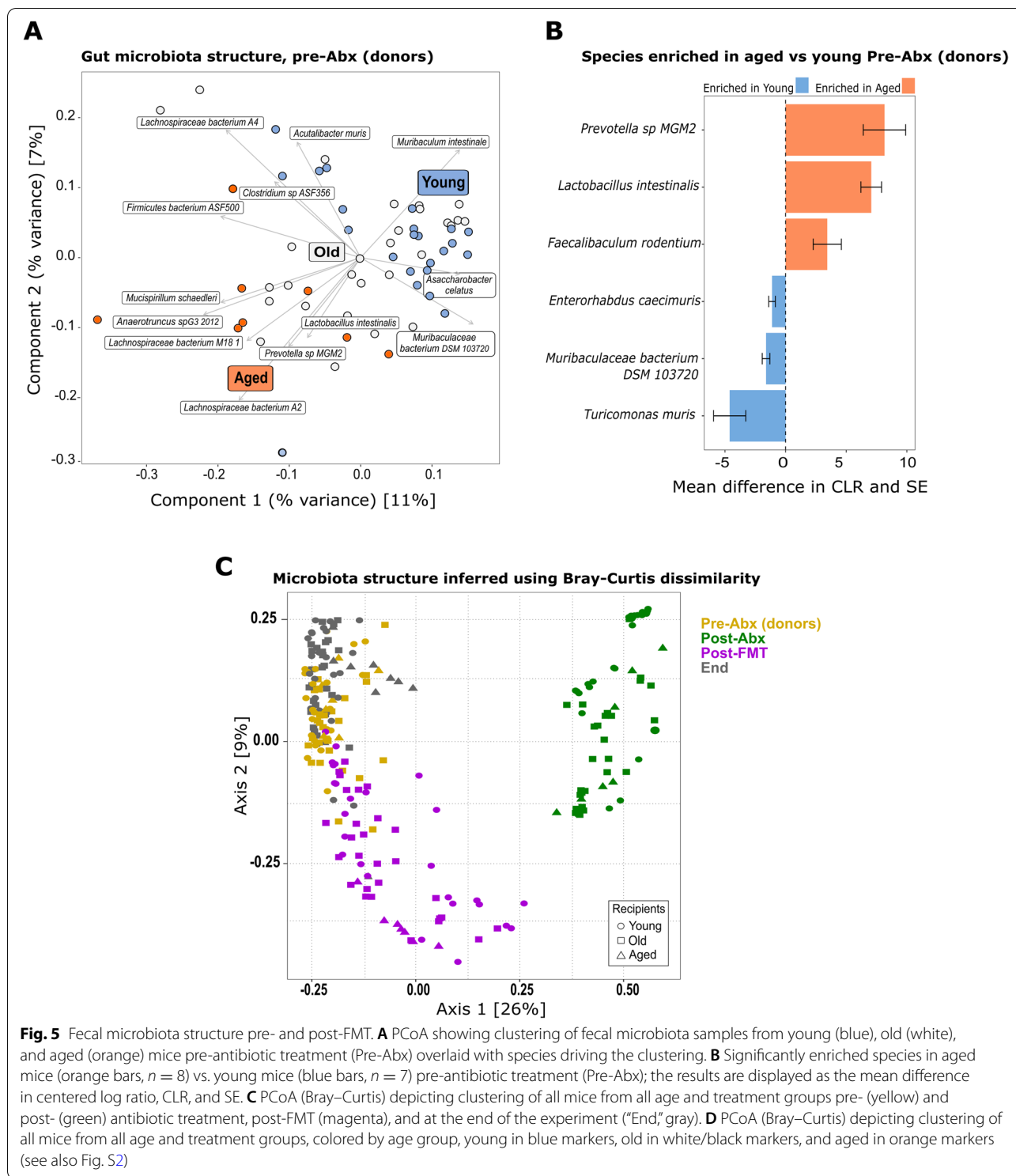
To identify specific changes in the gut microbiota with age, and following transplantation, we performed whole-genome shotgun (WGS) metagenomic sequencing of all mice at multiple time points. Prior to FMT, we first established the baseline taxonomy of the fecal microbiota of the young, old, and aged mice. Altered microbial beta diversity profiles were seen with age (Fig. 5A, Figs. S7 and S8), as noted previously in mice [64, 112, 118] and humans [19, 25, 26, 49, 86, 87]. We identified species which drove the clustering of the age groups (Fig. 5A), including *Muribaculaceae*, *Lacnospiraceae*, *Lactobacillus*, *Clostridium*, and *Prevotella* species. *Prevotella* sp., *Lactobacillus intestinalis*, and *Faecalibaculum rodentium* were significantly enriched in the aged vs. young groups whereas *Enterorhabdus caecimuris*, *Turicimonas muris*, and *Muribaculaeae* bacterium DSM 103720 were significantly enriched in the young vs. old group (Fig. 5B and Fig. S7). A pairwise PERMANOVA showed that the intestinal microbiota was significantly different between all age groups ($P < .01$ after Benjamini–Hochberg, BH correction). The young (3 months) and aged (24 months) groups formed separate clusters in the ordination; however, the old (18 months) group did not form a separate cluster and shared features with both young and aged mice (Fig. 5A, Fig. S8). Importantly, we accounted for potential inter-cage variability, both before FMT by randomizing housing in the weeks prior to the start of the experiment and post-FMT by factoring inter-cage variation into our statistical analyses of the metagenomic data.

Using FMT, we exchanged the fecal microbiota of young, old, and aged groups of mice as detailed in Fig. 1. Fecal pellets were collected pre- and post-antibiotic treatments and at 1 and 2 weeks post-FMT. Fecal microbial and metabolite compositions were assessed by metagenomic sequencing, metabolic pathway

abundance analysis, and NMR. Antibiotic pre-treatment, as expected, resulted in significant depletion of observed species across all treated groups of all ages (Fig. S2, Tukey post hoc test $P < .01$) and drastically altered the overall bacterial community composition in all age groups compared with pre-antibiotic treatment (Fig. 5C, green vs. yellow markers, 5D, S7 and S8). FMT restored the number of observed species to pre-antibiotic levels (Fig. S2). The FMT induced significant alterations in the fecal microbiota of recipients (Fig. 5C, D, Figs. S7 and S8, permutational ANOVA on dbRDA $F = 55.8$, $df = 3$, $P < .01$) with experimental time point accounting for 50% of the data variance ($R^2_{adj} = 50\%$). More importantly, heterochronic FMT between young and aged groups induced clear shifts in the recipient fecal microbiota composition, indicating successful divergence of the recipients' gut microbiota from its initial composition (pairwise PERMANOVA $P < .01$ after BH correction, Fig. 5C, magenta vs. yellow markers, and Fig. S7). This was most pronounced at the "Post-FMT" time point, whereas by the end of the study, there was a greater overlap with the original donor profiles (Fig. 5C, yellow vs. gray markers), suggesting that the recipients' intestinal environment strongly modulated long-term engraftment success.

The old (18 months) group of animals had significant inter-individual variation in the microbiota composition and did not form a discrete cluster in the ordination (Fig. 5A, Fig. S8). Therefore, we focused our further metagenomic analysis on the more divergent young and aged mice, and therein on detecting the major temporal shifts in microbiota structure by comparing the "Pre-Abx" and "Post-FMT" time points (Fig. 6). Transfer of aged donor microbiota into young mice dramatically altered the recipients' fecal microbiota composition (pairwise PERMANOVA $P = .01$, after BH correction) and resulted in a microbiota profile resembling that of aged mice at baseline (Fig. 6A). A significant compositional shift (pairwise PERMANOVA $P = .01$, after BH correction) was also induced in aged mice receiving young donor microbiota. In this case, the altered profile was distinct from that of young baseline mice, with the observed shifts following those of young mice transplanted with a young donor microbiota (Fig. 6A). This suggests that the aged donor microbiota engraftment was strongest in the young recipients, while the transfer of young donor microbiota was more susceptible to modification by the influence of the FMT procedure, or the recipient intestinal environment, or both.

Species belonging to the *Oscillibacter* and *Prevotella* genera, an unknown species in the Firmicutes phylum, and *Lactobacillus johnsonii* drove the clustering of aged mice and that of young mice transplanted with aged donor microbiota (Fig. 6A). In contrast, the divergence of



young mice receiving young donor microbiota and aged mice receiving young donor microbiota was driven by species within the genera *Bifidobacterium*, *Akkermansia*, *Parabacteroides*, *Clostridium*, and *Enterococcus* (Fig. 6A).

Members of the *Bifidobacteriaceae*, *Akkermansiaceae*, and *Eubacteriaceae* families that are associated with beneficial effects on intestinal and extra-intestinal health in both mice and humans ([8, 38, 43, 73, 78, 81]) were more

abundant in both young and aged recipients of young donor microbiota (Fig. S3A, differentially abundant families listed in Table S2).

Transplanting young mice with an aged donor microbiota resulted in enrichment of the signature species of the aged mice, namely *Prevotella* sp. MGM2, and *L. intestinalis*, along with *Lachnospiraceae* bacterium 10–1, *Parabacteroides distasonis*, and *L. johnsonii* (Fig. 6A, B).

Conversely, transplanting aged mice with a young donor microbiota resulted in enrichment of signature species of the young mice, *T. muris* and *Muribaculaceae* bacterium DSM103720, along with *Bifidobacterium animalis*, *Eubacterium* sp14–2, *Akkermansia muciniphila*, and six other species (Fig. 6A, B). *Enterorhabdus caecimuris*, although slightly enriched in young mice, was not significantly enriched in aged mice receiving young donor microbiota (Fig. 6A, B).

The most significantly enriched species in aged mice receiving young donor microbiota (*Bifidobacterium animalis*, *Eubacterium* sp. 14–2, *A. muciniphila*, and *Clostridium cocleatum*) were also enriched in young mice recolonized with young donor microbiota, although others (*Parabacteroides distasonis*, *Lachnospiraceae* 28–4, *Clostridium* ASF356) were only enriched in the aged recipients (Fig. 6B and Fig. S3B), consistent with an impact of the recipient intestinal environment on engraftment success of different species.

We confirmed that enriched species in aged mice receiving young donor FMT did not reflect only those species which were not eliminated, or were better able to flourish after antibiotic treatment, by cross-checking against species which were enriched post-antibiotics only in controls (Fig. S3C). A table of differentially abundant species is provided in Table S1.

Collectively, our results showed that heterochronic FMT resulted in significant alteration of the recipient microbiota structure, enriching for bacterial species distinctive of the donor age group, and that both donor and recipient were influential in the resulting microbiota composition.

To estimate whether the FMT interventions altered potential microbial functional profiles in recipients, and to identify potential molecular mediators of the effects seen in the gut, brain, and retina, we next analyzed microbial metabolic pathway abundance in the WGS data to infer functional capacity and, in parallel, analyzed

fecal metabolite concentrations by NMR in young and aged mice pre- and post-FMT.

Heterochronic FMT alters lipid and vitamin metabolism

Microbial metabolites are key mediators of microbiota function and influencers of host cell physiology and metabolism. Targeted nuclear magnetic resonance ($^1\text{H-NMR}$) spectroscopy-based metabolomics of fecal samples from young and aged mice, pre- and post-heterochronic FMT, was performed primarily to assess amino acids, sugars, short-chain fatty acids (SCFA), and alcohols (the metabolites detected, and their raw concentrations are detailed in Table S3). Distance-based redundancy analysis (dbRDA) showed high inter-individual variation with only 24% of variance explained by treatment groupings (4% of variance was explained by cage groupings). Permutational ANOVA on the modeling suggested significant differences among the groups ($F = 2.27$, $df = 3$, $P = .003$). However, subsequent pairwise PERMANOVA comparisons on the Euclidean distance matrix found no statistically significant differences between any two groups ($.05 < P < .1$ after BH correction).

Using a partial least squares-discriminant analysis (PLS-DA), we identified metabolites with the strongest influence on defining the separation between groups (Figs. S4A and S4B). Overall, metabolic profiles were broadly similar, with only a limited degree of variation in some metabolites across age and treatment groups. In young mice receiving aged donor microbiota, these included metabolites involved in amino acid metabolism (malate threonine and creatine) and sugar metabolism (fucose and sucrose). In aged mice receiving young donor microbiota, the greatest contributors to the loadings were tauro-conjugated bile acids, acetate, the polyamine putrescine, and polyamine regulator ornithine, metabolites previously associated with beneficial effects in aging [74, 94].

In parallel, we analyzed functional metabolic pathway abundances in the metagenomic data. In aged mice receiving young donor microbiota, we detected significant enrichment of multiple pathways involved in lipid synthesis compared with pre-transfer samples (Fig. 7A) and, in particular, pathways involved in the synthesis of medium- and long-chain fatty acids (MCFA, LCFA). Significantly, some of these lipid metabolism pathways were depleted in young mice receiving aged donor microbiota, including biosynthesis of palmitate, mycolate, and

(See figure on next page.)

Fig. 6 Donor-derived species define the fecal microbiota composition of FMT recipients. **A** PCoA showing clustering of fecal microbiota samples from young and aged mice Pre-Abx (green) and post-FMT (orange), and overlaid with species driving the clustering. **B** Differential abundance analysis (results displayed as the mean difference in centered log ratio, CLR, and SE) of enriched species post-heterochronic transfer (Post-FMT) vs. pre-transfer (Pre-Abx) in young and aged mice. Family abundance, young mice receiving coeval transfer, and antibiotic-only groups shown in Fig. S3

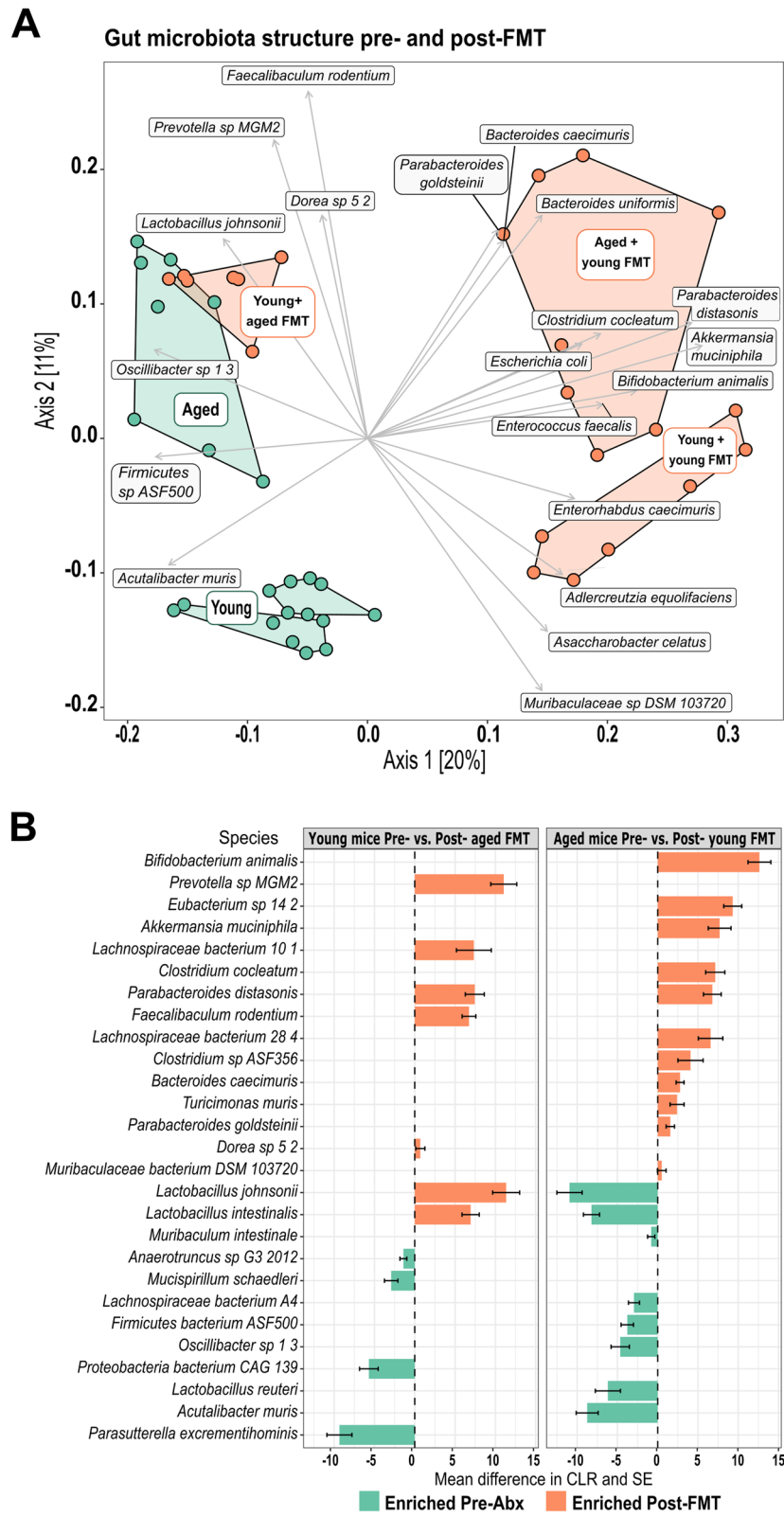
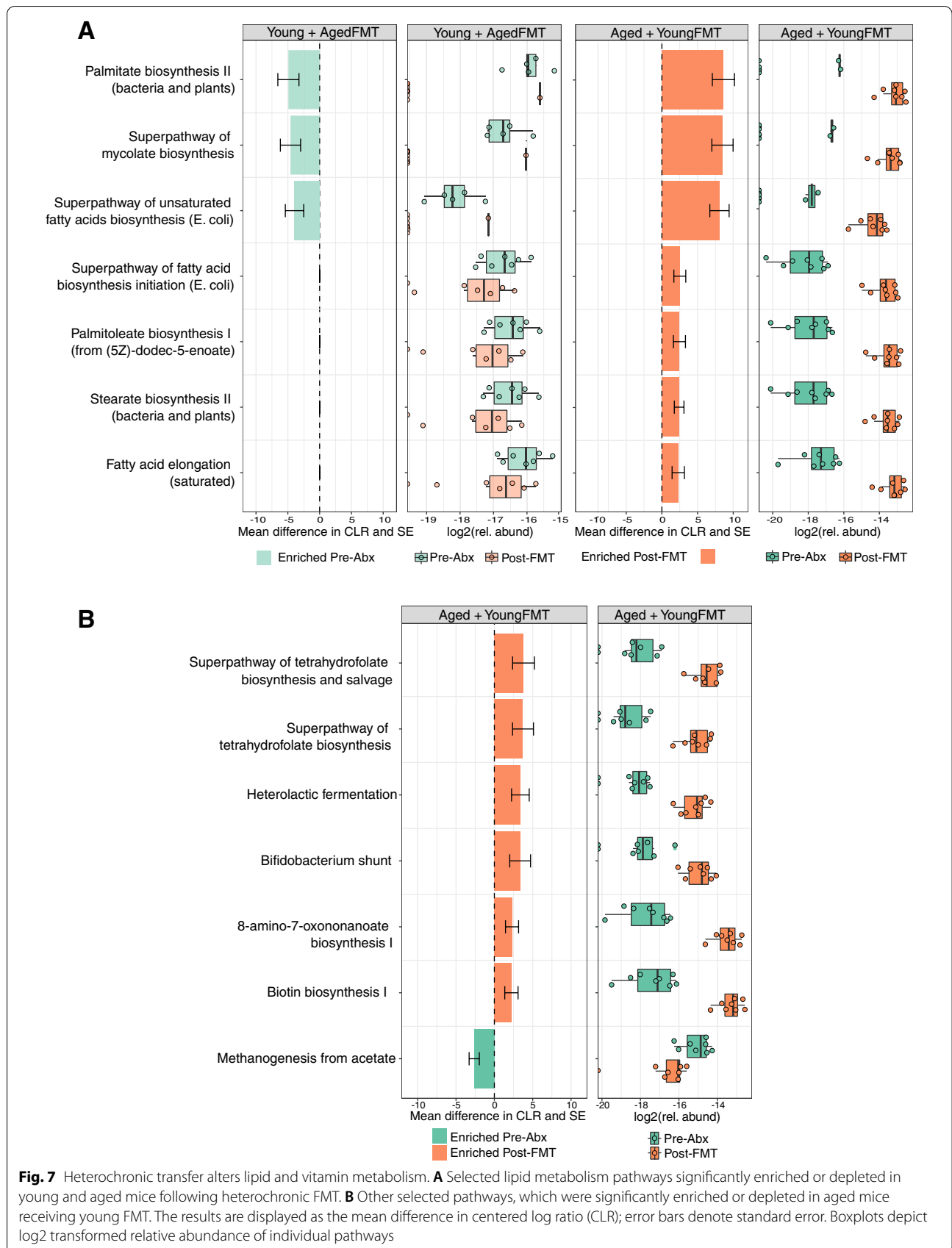


Fig. 6 (See legend on previous page.)



unsaturated fatty acids. Other pathways enriched in aged mice transplanted with young donor microbiota included those involved in the biosynthesis of the vitamins B7 and B9 (biotin and folate) (Fig. 7B). There was also a reduction in methanogenesis suggestive of some impact on gut archaea, an increase in heterolactic fermentation, utilized by some *Lactobacillus* species, and an increase in the *Bifidobacterium* shunt pathway (Fig. 7B), the latter in keeping with the increase in proportional abundance of *Bifidobacterium* spp. in this group (Fig. 6B). A full list of differentially enriched metabolic pathways pre- and post-FMT is provided in Table S4.

In summary, heterochronic FMT resulted in significant shifts in lipid and vitamin metabolism pathways, increasing their proportional abundance in aged mice transplanted with the microbiota of young donors and decreasing their abundance in young mice receiving aged donor microbiota. We also identified enrichment of heterolactic fermentation and *Bifidobacterium* shunt in aged mice receiving young donor FMT.

Discussion

Altered intestinal microbiota composition in old age is associated with chronic low-grade inflammation and increasing susceptibility to age-associated chronic diseases. However, whether age-associated changes in the diversity, composition, or function of the gut microbiota are causal in disease etiology remains largely unknown. Here, we used FMT between young and aged mice, to bi-directionally modulate recipient microbiota structure and metabolic capability. We show that aged donor microbiota transfer to young mice drives inflammation and loss of integrity in the intestinal epithelial barrier elevated systemic and tissue markers of inflammaging, and upregulated inflammation in the retina and brain. The transferred aged microbiota and resulting recipient microbiota composition were distinguished by enrichment for *Prevotella*, *Lacnospiraceae*, and *Facecalibaculum* species and depletion of long-chain fatty acid synthesis. Conversely, transfer of aged mice with young donor microbiota, which was distinguished by enrichment *Bifidobacteria*, *Eubacteria*, and *Akkermansia* species, and enrichment for B vitamin biosynthesis and lipid synthesis pathways reversed inflammatory changes in the aged gut, brain, and retina. Our data support the suggestion that altered gut microbiota in old age contributes to intestinal and systemic inflammation, and so may contribute to driving inflammatory pathologies of aged organs. Targeting the gut–brain axis in aging, by modification of microbial composition to modulate immune and metabolic pathways, may therefore be a potential avenue for therapeutic approaches to age-associated inflammatory and functional decline.

Signature microbes of the aging GI tract pre- and post-FMT

We identified age-associated signature bacteria which, after transfer by heterochronic FMT, become prominent within the recipients' engrafted microbiota. Importantly, this analysis accounted for any potential inter-cage variability, by factoring inter-cage variation into our statistical analyses. In all animals, the shift in microbial structure induced by heterochronic FMT was most apparent at 7 days post-FMT. By 18 days post-FMT, the transplanted microbiota more closely resembled the baseline, pre-antibiotic treatment microbiota profile (correlation in a symmetric Procrustes rotation = 25%, $P = .05$). This suggests that age and environmental factors in the GI tract of the recipient provide particular ecological niches favoring specific bacterial taxa.

This adaptation over time however did not limit the impact of the transplanted microbiota on tissues, in which changes in key functional cell types and biomarkers of health were apparent at 18 days post-FMT, the point of tissue collection. This raises the question of the stability of the engrafted microbiota and whether long-term persistence is necessary to maintain beneficial health effects, which could be addressed in larger long-term studies.

In both aged mice and in young recipients of aged donor microbiota, we saw significant enrichment of *Prevotella* sp_MGM2. *Prevotella* species associated with detrimental impacts on intestinal barrier integrity are enriched in IBS patients and in models of intestinal inflammation [52, 113] and may promote inflammatory arthritis [3, 104, 126]. However, other reports identify beneficial impacts of *Prevotella* species on glucose metabolism [60], and there are conflicting associations with Parkinson's disease progression [97].

Bifidobacterium animalis and *Akkermansia muciniphila* were among the most enriched taxa in young mice and in aged mice receiving a young donor microbiota and are associated with promoting intestinal and extra-intestinal health and healthy aging. Furthermore, *A. muciniphila* is depleted in models of inflammation and metabolic disorders and displays probiotic potential, by regulating mucus production and epithelial barrier integrity and by reducing serum LPS [38]. This latter impact on LPS is in accordance with the reduced serum LBP levels we saw in young mice and aged mice receiving young donor microbiota. In mouse models of accelerated aging, supplementation with *A. muciniphila* can also attenuate age-related decline in colon thickness and immune activation [73], and exert beneficial effects on lifespan and healthspan [8].

Other species we found enriched in aged recipients of young donor microbiota included *B. animalis*, a probiotic species positively associated with longevity in mice [78] and negatively correlated with inflammation and human obesity [81], and *Eubacterium* sp. 14–2. The precise classification of many species within the *Eubacteriaceae* family is under review. However, some species are currently thought

to modulate cholesterol and bile acid metabolism and are considered potential therapeutics [43].

Overall, our data indicate that FMT with microbiota from young mice leads to an enrichment of beneficial taxa in aged mice. Refined colonization studies using single species, or defined consortia, would help to define the contributions of particular taxa to the systemic effects we have described, and to identify their specific mechanisms of action. It also remains unknown whether specific microbial species mediate their effects through unique bacterial products, or by expansion and potential colonization of new niches. Our procedures were optimized to assess the bacterial fraction of the intestinal microbiota, and as such, we cannot exclude potential contributions from other microbial constituents in the effects we describe. The identification of small differences in the abundance of the methanogenesis pathway following FMT suggests a possible shift in archaeal metabolism or abundance between our treatment groups; however, further investigation to evaluate this and other components, which may have significant impacts on host health, will require the use of additional protocols optimized for fungal [53], viral [30, 34], and archaeal [77] extraction and identification.

The aged intestinal microbiota drives barrier permeability and inflammation

A central question regarding inflammaging and age-associated intestinal pathology is whether breakdown of epithelial barrier integrity and function drives changes in the intestinal microbiota, or, whether a shift in microbiota composition leads to epithelial damage and permeability, or if both occur concomitantly [2, 128]. Our data show that transplanting an aged donor microbiota into young recipients results in elevated intestinal concentrations of TNF, and elevated surrogate biomarkers of altered epithelial barrier permeability (I-FABP, LBP), supporting a driving role for the age-associated microbiota in the breakdown of barrier integrity and promotion of systemic inflammatory responses. That these effects are reversed in aged recipients of young donor microbiota supports this hypothesis, suggesting a positive impact of the microbiota of young mice on barrier integrity, or that removal of age-associated microbiota allows for barrier recovery. In agreement with our findings and interpretation is the observation that the microbiota from aged donors exacerbates paracellular permeability and inflammation in germ-free mice [40, 118].

The intestinal microbiota regulates CNS microglia activation

In mammalian models, altered microglial morphology and function, and elevated expression of microglial

activation markers are seen with advancing age [82]. However, it is unclear whether age and absolute numbers of activated microglia in different regions of the brain are positively associated. Here, we observed higher numbers of Iba-1⁺ microglia in both the corpus callosum and the cortex with age in healthy mice. Further, we show that Iba1⁺ cell density in both regions is regulated by the age-associated gut microbiota. Transplanting young donor microbiota reduced elevated numbers of Iba-1⁺ microglia in the CNS of aged recipients, while aged donor microbiota increased Iba-1⁺ cells in the CNS of young recipients. These striking changes in microglia activation could reflect expansion and/or contraction in total microglial cell number, or modulation of Iba-1⁺ expression in resident populations, or both. CNS microglial populations constantly and rapidly remodel [6], making it difficult to discriminate between changes in cell number versus changes in Iba-1 expression in the setting of FMT. Long-term imaging, lineage-tracing mouse models, and pulse-chase studies would be useful in addressing these distinctions.

Loss of intestinal barrier integrity and elevated circulating pro-inflammatory cytokine concentrations are linked with the polarization of CNS microglia toward a pro-inflammatory phenotype [11, 73, 109] and promote neurodegenerative disease [10, 13, 48]. In accordance with these data, we saw disrupted barrier integrity and increased bacterial translocation following the transfer of aged donor microbiota into young recipients.

Modulation of metabolism is another way in which FMT may impact microglial activation. Here, we found lipid metabolism pathways were significantly altered by heterochronic FMT, particularly in aged mice receiving young donor microbiota. Evidence for unsaturated, mono-, and poly-unsaturated fatty acids impacting microglial function comes from both in vitro and in vivo studies [70]. Palmitate, for example, which here was enriched in the aged mice receiving young donor microbiota, has anti-inflammatory effects in microglial cells [58, 80, 119]. Targeted metabolomics approaches and regional sampling would aid further investigation by determining levels of specific metabolites identified by our analysis along the GI tract. Other possible mediators of FMT impacts on CNS inflammation include inflammatory cytokine signaling and immunomodulatory factors induced by members of the microbiota and gut–brain transport of microbial products including microvesicles which can cross the blood–brain barrier [45, 47, 124]. Of note, Iba-1 numbers also appeared reduced in antibiotic-treated mice, suggesting that depletion or elimination of detrimental species, may be more significant in regulating microglial inflammation than the introduction of beneficial species. The antibiotics used in

this study are, to varying degrees, able to penetrate the blood–brain barrier and cerebrospinal fluid. It is therefore theoretically possible that treatment with antibiotics could also affect microglial reactivity in the brain by depleting any local CNS-associated microbes, although the existence of a brain-associated microbiome remains highly controversial.

Young mice transplanted with an aged donor microbiota display defects in spatial learning and memory [33], suggesting the possibility that in the reverse situation, young donor FMT to aged mice could potentially have beneficial impacts on cognitive measures. However, both this study and a recent study also using young donor FMT in aged mice [15] showed no beneficial effect of transplantation with young donor fecal microbiota using behavioral tests of short-term spatial learning and memory. Longer-term assessment using the Morris Water Maze test of aged mice following repeated young donor FMT over 4 weeks did show some improvement for aged recipients of young vs. aged donor FMT [15], suggesting that impacts on behavior may require more subtle analysis and that substantially altering behavioral phenotypes may require sustained microbial intervention. Extrapolating the relevance of our findings to co-morbidities of aging in humans would require comparable FMT studies in elderly individuals. There is some evidence for improved cognition with probiotic use in those with pre-existing cognitive impairment [31], although the utility and effectiveness of single or small consortia of beneficial microbes in modulating age-associated neuro-inflammatory and retinal diseases remain to be determined.

The intestinal microbiota regulates retinal inflammation

Association studies have linked intestinal microbial products with the development and progression of age-related choroidal neovascularization (CNV) and age-related macular degeneration (AMD) [4, 131, 133]. Here, we provide the first direct evidence that aged intestinal microbiota drives retinal inflammation and regulates expression of the functional visual protein RPE65 at the RPE/BM interface. Polymorphisms in human complement regulatory factor H (CFH) predispose individuals to AMD [35, 46, 59] and CFH deficiency in mice causes retinal abnormalities, including accumulation of complement C3, resulting in significant visual dysfunction [28]. We found high levels of C3 expression in aged mice were reversed after receiving a young donor microbiota. Conversely, transplanting an aged donor microbiota into young mice resulted in elevated levels of retinal C3 expression, comparable to levels in aged mice. RPE65 is vital for maintaining normal photoreceptor function via trans-retinol conversion; mutations or loss of function are associated with retinitis pigmentosa and are implicated in AMD

[21]. Our finding that age-associated decline in host retinal RPE65 expression is induced by an aged donor microbiota, and conversely is rescued by young donor microbiota transfer, suggests age-associated gut microbiota functions or products regulate visual function.

Retinal degeneration induces upregulation of a cytokine and chemokine production whose expression is coordinated by Müller cells, microglia, and RPE [102]. Transfer of young donor microbiota results in a decrease in aged mice of cytokines involved in inflammatory immune cell recruitment and pro-inflammatory signaling, including CCL11 (eotaxin), CXCL11, and IL-1 β [23, 62, 84], all of which are elevated in aged mouse retinae [108]. Elevated CCL11 in the plasma and cerebrospinal fluid seen in aging mice and humans are associated with declining neurogenesis, neurodegenerative disease, and cognitive decline and may contribute to driving neovascularisation in AMD via interaction with CCR3 [1, 93, 123]. Upregulation of CXCL11 is seen in RPE cells adjacent to drusen deposits in AMD [62], and its secretion can be triggered by proinflammatory cytokines including TNF and IL-1 β . In addition, IL-1 β is associated with the progression of retinal pathologies, including AMD [130]. Together, our results show that transfer of young microbiota to aged mice reduces the expression of key cytokines associated with driving inflammation and disease in the retina.

One plausible scenario by which the microbiota influences complement expression in the retina is that these changes are a consequence of leakage of microbial products from the gut into the systemic circulation and/or upregulation of systemic inflammatory cytokine signaling, in both aged mice and in young mice treated with aged donor FMT. This is particularly impactful on tissues such as the retina with high metabolic and circulatory input and demand. It is also possible that upregulated complement expression by the liver as part of an acute phase response to bacterial toxins in the blood, as supported by our finding that heterochronic FMT altered circulating LBP levels, leads to accumulation of complement proteins at retinal membranes.

Our metagenomic pathway analysis identified a positive impact of young donor microbiota on key vitamins important for maintaining eye health during aging. Vitamin B synthesis pathways, important in photoreceptor maintenance and regulation of retinal vascular health, were enriched in aged recipients of young donor microbiota, while being depleted in young recipients of aged donor microbiota. Deficiencies in B vitamins are implicated in retinitis pigmentosa and glaucoma, for which improved outcomes can be achieved by dietary supplementation [24, 114]. It is currently unclear how much of the B vitamin production by gut microbiota is accessible by the host; however, our results suggest that microbial

modulation, combined with dietary or pharmacological supplementation of B vitamin levels to modulate retinal RPE65 expression, could have potential therapeutic value in the treatment of retinal diseases and in general maintenance of eye health in old age.

Conclusions

Our results demonstrate that the age-associated changes in the murine intestinal microbiota contribute to disrupted gut barrier integrity and systemic and tissue inflammation affecting the retina and the brain, but these changes can be reversed by replacement with young donor microbiota. Further work to assess the long-term persistence of the beneficial effects of young donor microbiota transfer, in the eye and brain, will establish whether FMT can promote long-term health benefits in aged individuals and ameliorate age-associated neurodegeneration and retinal functional deterioration.

Abbreviations

Abx: Antibiotics; AMD: Age-related macular degeneration; BM: Bruch's membrane; C3: Complement component 3; CNS: Central nervous system; FMT: Fecal microbiota transplant; GI: Gastrointestinal; Iba-1: Ionized calcium-binding adaptor protein 1; I-FABP: Intestinal fatty acid-binding protein; LBP: Lipopolysaccharide-binding protein; LPS: Lipopolysaccharide; NGS: Next-generation sequencing; NMR: Nuclear magnetic resonance; PBS: Phosphate-buffered saline; RPE: Retinal pigment epithelium; RPE65: Retinal pigment epithelium-specific 65 kDa protein; (S/M/L) CFA: Short-, medium-, long-chain fatty acids; SPF: Specific pathogen-free; TNF: Tumor necrosis factor; WGS: Whole-genome shotgun.

Supplementary Information

The online version contains supplementary material available at <https://doi.org/10.1186/s40168-022-01243-w>.

Additional file 1: Table S1. Differential abundance table (species). Relates to Fig. 6B and Figure S3B. Provided as a separate Excel file.

Additional file 2: Table S2. Differential abundance table (family). Relates to Figure S3A. Provided as a separate Excel file.

Additional file 3: Table S3. Raw fecal metabolite concentrations from NMR analysis. Relates to Figure S4. Provided as a separate Excel table.

Additional file 4: Table S4. Full list of differentially abundant metabolic pathways Pre- vs. Post-FMT. Relates to Fig. 7. Provided as a separate Excel file.

Additional file 5: Figure S1. Related to Fig. 2. Iba-1⁺ cell density in corpus callosum is regulated by the intestinal microbiota. (A) Iba-1⁺ microglia were identified by immunostaining (red), nuclei counterstained with Hoechst (blue) in the corpus callosum (highlighted in cartoon) of sagittal brain sections. (B) Representative immunostaining of young, old, and aged mice, either treated with PBS only, treated with antibiotics (Abx) only, or with antibiotics followed by FMT from young, old, or aged donors. Quantified in Fig. 2. **Figure S2.** Related to Fig. 5. Impact of antibiotics and microbiota transfers on observed species. Number of observed bacterial species pre- and post-antibiotic treatment, post-FMT and at the end of the experiment. Pairwise comparison, Kruskal-Wallis, * = $P < .0001$. **Figure S3.** Related to Fig. 6. Clustering of beta-diversity post-FMT is driven by donor age, and differential abundance of bacterial families identified pre- and post-transfer. (A) Differential abundance of bacterial families in aged mice receiving young donor microbiota, and in young mice

receiving young, old, or aged donor microbiota. (B) Species enriched in the young mice receiving young donor microbiota. (C) Microbiota surviving/enriched post-antibiotics only. **Figure S4.** Metabolite profiles in fecal pellets estimated by (1 H)-NMR. (A) PLS-DA comparing fecal metabolite profiles (full list of metabolites in Supplementary Table S3) of young and aged groups pre- and post-heterochronic transfer estimated by NMR. (B) Specific metabolites contributing to the loading of component 1, 2, and 3 in the PLS-DA analysis. **Figure S5.** Behavioral testing in aged mice shows no difference between aged mice receiving young vs. aged donor FMT. (A) Novel object recognition (NOR) test and (B) Y-maze test results for: young mice (n = 11), aged mice (n = 20), aged mice + young donor FMT (Y-FMT) (n = 10) and aged mice + aged donor FMT (A-FMT) (n = 10). Error bars denote 95% CI. **Figure S6.** Per-sample read numbers in metagenomic sequencing data. (A) Beeswarm plot, (B) histogram, and (C) scatter plot, depicting per-sample read numbers in trimmed and decontaminated metagenomic sequencing data. Samples from all mice from all groups. **Figure S7.** Bubble plot depicting variation between metagenomic samples across mice within young and aged groups pre- and post-FMT. **Figure S8.** Bubble plot depicting variation between metagenomic samples across mice within old groups pre- and post-FMT.

Additional file 6. Key Resources Table.

Acknowledgements

We thank the staff of the Disease Modelling Unit at the University of East Anglia for animal husbandry and ensuring animal welfare. We also thank Dr. Sergey Nepogodiev for the assistance with NMR and Professor Alan Walker and Dr. Judith Pell for the comments on the manuscript.

Data and code availability

The metagenomic sequencing raw reads generated during this study are freely available at SRA (<https://www.ncbi.nlm.nih.gov/sra/>) under accession number PRJNA706366. Code: The R code generated to analyze the metabolomic and metagenomic data in this study is available at https://github.com/StfnRomano/Parker_et_al_Inflammaging.

Authors' contributions

AP: conceptualization, methodology, investigation, formal analysis, data visualization, and manuscript original draft: review and editing. SR: data curation, formal analysis, investigation, methodology and code development, data visualization, and manuscript original draft: review and editing. RA: data curation and methodology. AA: investigation and data visualization. GLG: investigation and formal analysis. GMS: formal analysis, methodology, and manuscript review and editing. MP: investigation and formal analysis. AT: data curation. EJ: sample acquisition and manuscript review. DV: methodology and interpretation of the data. DB and SR: investigation. LAB: supervision and manuscript review and editing. GJ: conceptualization, supervision, resources, funding, and manuscript review and editing. SRC: conceptualization, supervision, resources, funding, project administration, and manuscript review and editing. The authors read and approved the final manuscript.

Funding

The authors gratefully acknowledge the support of the Biotechnology and Biological Sciences Research Council (BBSRC); this research was funded by BBSRC Core Capability Grant BB/CCG1860/1, project grant BB/N000250/1, and BBSRC Institute Strategic Programme Grant Gut Microbes and Health (BB/R012490/1) and its constituent projects BBS/E/F/000PR10353, BBS/E/F/000PR10355, and BBS/E/F/000PR10356.

Availability of data and materials

Further information and requests for resources and reagents should be directed to, and will be fulfilled by, the lead contact, Simon R. Carding (simon.carding@quadram.ac.uk).

Declarations

Ethics approval and consent to participate

All experiments involving animals were performed in accordance with EU and United Kingdom Home Office Legislation, revised Animals (Scientific

Procedures) Act 1986 UK, and following local Animal Welfare and Ethical Review Body approval.

Consent for publication

Not applicable.

Competing interests

The authors declare that they have no competing interests.

Author details

¹Gut Microbes and Health Research Programme, Quadram Institute, Norwich NR4 7UQ, UK. ²Institute of Ophthalmology, University College London, London EC1V 9EL, UK. ³Norwich Medical School, University of East Anglia, Norwich NR4 7TJ, UK.

Received: 3 December 2021 Accepted: 4 February 2022

Published online: 29 April 2022

References

- Takeda A, Baffi JZ, Kleinman ME, Cho WG, Nozaki M, Yamada K, et al. CCR3 is a target for age-related macular degeneration diagnosis and therapy. *Nature*. 2009;460(7252):225–30. <https://doi.org/10.1038/NATURE08151>.
- Aleman FDD, Valenzano DR. "Microbiome evolution during host aging." edited by John M. Leong. *PLoS Pathog*. 2019;15(7):e1007727. <https://doi.org/10.1371/journal.ppat.1007727>.
- Alpizar-Rodriguez D, Lesker TR, Gronow A, Gilbert B, Raemy E, Lamacchia C, et al. *Prevotella copri* in individuals at risk for rheumatoid arthritis. *Ann Rheum Dis*. 2019;78(5):590–3. <https://doi.org/10.1136/annrheumdis-2018-214514>.
- Andriessen EMMAMA, Wilson AM, Mawambo G, Dejda A, Miloudi K, Sennlaub F, et al. Gut microbiota influences pathological angiogenesis in obesity-driven choroidal neovascularization. *EMBO Mol Med*. 2016;8(12):1366–79. <https://doi.org/10.15252/emmm.201606531>.
- Arbizu, PM. 2020. "PairwiseAdonis: pairwise multilevel comparison using Adonis. R Package Version 0.4." <https://github.com/pmartinezarbizu/pairwiseAdonis>.
- Askew K, Li K, Olmos-Alonso A, Garcia-Moreno F, Liang Y, Richardson P, et al. Coupled proliferation and apoptosis maintain the rapid turnover of microglia in the adult brain. *Cell Rep*. 2017;18(2):391–405. <https://doi.org/10.1016/j.celrep.2016.12.041>.
- Balaratnasingam C, Yannuzzi LA, Curcio CA, Morgan WH, Querques G, Capuano V, et al. Associations between retinal pigment epithelium and drusen volume changes during the lifecycle of large drusenoid pigment epithelial detachments. *Investig Ophthalmol Vis Sci*. 2016;57(13):5479–89. <https://doi.org/10.1167/iov.16-19816>.
- Bárceña C, Valdés-Mas R, Mayoral P, Garabaya C, Durand S, Rodríguez F, et al. Healthspan and lifespan extension by fecal microbiota transplantation into progeroid mice. *Nat Med*. 2019;25(8):1234–42. <https://doi.org/10.1038/s41591-019-0504-5>.
- Bates D, Mächler M, Bolker BM, Walker SC. Fitting linear mixed-effects models using lme4. *J Stat Softw*. 2015;67(1):1–48. <https://doi.org/10.18637/jss.v067.i01>.
- Becker L, Nguyen L, Gill J, Kulkarni S, Pasricha PJ, Habtezion A. Age-dependent shift in macrophage polarisation causes inflammation-mediated degeneration of enteric nervous system. *Gut*. 2018;67(5):827–36. <https://doi.org/10.1136/gutjnl-2016-312940>.
- van Beek AA, Van Bossche J, Mastroberardino PG, de Winther MPJ, Leenen PJM. Metabolic alterations in aging macrophages: ingredients for inflammaging? *Trends Immunol*. 2019a. <https://doi.org/10.1016/j.it.2018.12.007>.
- Beghini F, Mciver LJ, Blanco-Míguez A, Dubois L, Asnicar F, Maharjan S, et al. Integrating taxonomic, functional, and strain-level profiling of diverse microbial communities with BioBakery 3. *BioRxiv*. 2020:19.388223. <https://doi.org/10.1101/2020.11.19.388223>.
- Bevan-Jones WR, Cope TE, Simon Jones P, Kaalund SS, Passamonti L, Allinson K, et al. Neuroinflammation and protein aggregation co-localize across the frontotemporal dementia spectrum. *Brain J Neurol*. 2020;143(3):1010–26. <https://doi.org/10.1093/brain/awaa033>.
- Blazes M, Lee CS. Understanding the brain through aging eyes. *Adv Geriatr Med Res*. 2021;3(2). <https://doi.org/10.20900/AGMR20210008>.
- Boehme M, Guzzetta KE, Bastiaanssen TFS, van de Wouw M, Moloney GM, Gual-Grau A, et al. Microbiota from young mice counteracts selective age-associated behavioral deficits. *Nature Aging*. 2021;1(8):666–76. <https://doi.org/10.1038/s43587-021-00093-9>.
- Boehme M, van de Wouw M, Bastiaanssen TFS, Olavarria-Ramirez L, Lyons K, Fouhy F, et al. Mid-life microbiota crises: middle age is associated with pervasive neuroimmune alterations that are reversed by targeting the gut microbiome. *Mol Psychiatry*. 2019. <https://doi.org/10.1038/s41380-019-0425-1>.
- Boulangé CL, Neves AL, Chilloux J, Nicholson JK, Dumas ME. Impact of the gut microbiota on inflammation, obesity, and metabolic disease. *Genome Med*. 2016. <https://doi.org/10.1186/s13073-016-0303-2>.
- Buchfink B, Xie C, Huson DH. Fast and sensitive protein alignment using DIAMOND. *Nat Methods*. 2014. <https://doi.org/10.1038/nmeth.3176>.
- Buford TW. (dis)trust your gut: the gut microbiome in age-related inflammation, health, and disease. *Microbiome*; 2017. <https://doi.org/10.1186/s40168-017-0296-0>.
- Bushnell, Author, Brian Bushnell, Rob Egan, Alex Copeland, Brian Foster, Alicia Clum, Hui Sun, et al. 2014. BBMap: a fast, accurate, splice-aware aligner. <https://doi.org/10.1186/1471-2105-13-238>.
- Cai X, Conley SM, Naash MI. RPE65: role in the visual cycle, human retinal disease, and gene therapy. *Ophthalmic Genet*. 2009. <https://doi.org/10.1080/13816810802626399> NIH Public Access.
- Chen M, Muckersie E, Forrester JV, Heping X. Immune activation in retinal aging: a gene expression study. *Investig Ophthalmol Vis Sci*. 2010;51(11):5888–96. <https://doi.org/10.1167/iov.09-5103>.
- Cherry JD, Stein TD, Tripodis Y, Alvarez VE, Huber BR, Rhoda A, et al. CCL11 is increased in the CNS in chronic traumatic encephalopathy but not in Alzheimer's disease. *PLoS One*. 2017;12(9):e0185541. <https://doi.org/10.1371/JOURNAL.PONE.0185541>.
- Chou T-H, Romano GL, Amato R, Porciatti V. Nicotinamide-rich diet in DBA/2J mice preserves retinal ganglion cell metabolic function as assessed by PERG adaptation to flicker. *Nutrients*. 2020;12(7):1910. <https://doi.org/10.3390/nu12071910>.
- Claesson MJ, Cusack S, Sullivan O, O, Greene-Diniz R, De Weerd H, Flannery E, et al. Composition, variability, and temporal stability of the intestinal microbiota of the elderly. *Proc Natl Acad Sci U S A*. 2011;108(SUPPL. 1):4586–91. <https://doi.org/10.1073/pnas.1000097107>.
- Claesson MJ, Jeffery IB, Conde S, Power SE, O'connor EM, Cusack S, et al. Gut microbiota composition correlates with diet and health in the elderly. *Nature*. 2012;488(7410):178–84. <https://doi.org/10.1038/nature11319>.
- Clark RI, Salazar A, Yamada R, Fitz-Gibbon S, Morselli M, Alcaraz J, et al. Distinct shifts in microbiota composition during drosophila aging impair intestinal function and drive mortality. *Cell Rep*. 2015;12(10):1656–67. <https://doi.org/10.1016/j.celrep.2015.08.004>.
- Coffey PJ, Gias C, McDermott CJ, Lundh P, Pickering MC, Sethi C, et al. Complement factor H deficiency in aged mice causes retinal abnormalities and visual dysfunction. *Proc Natl Acad Sci U S A*. 2007;104(42):16651–6. <https://doi.org/10.1073/pnas.0705079104>.
- Combadière C, Feumi C, Raoul W, Keller N, Rodéro M, Pézard A, et al. CX3CR1-dependent subretinal microglia cell accumulation is associated with cardinal features of age-related macular degeneration. *J Clin Invest*. 2007;117(10):2920–8. <https://doi.org/10.1172/JCI31692>.
- Conceição-Neto N, Zeller M, Lefrère H, De Bruyn P, Beller L, Dehoutte W, et al. Modular approach to customise sample preparation procedures for viral metagenomics: a reproducible protocol for virome analysis. *Sci Rep*. 2015;5(1):1–14. <https://doi.org/10.1038/srep16532>.
- Coutts L, Ibrahim K, Tan QY, Lim SER, Cox NJ, Roberts HC. Can probiotics, prebiotics and synbiotics improve functional outcomes for older people: a systematic review. *Eur Geriatr Med*. 2020. <https://doi.org/10.1007/s41999-020-00396-x> Springer Science and Business Media Deutschland GmbH.
- Cui H, Tang D, Garside GB, Zeng T, Wang Y, Tao Z, et al. Wnt signaling mediates the aging-induced differentiation impairment of intestinal stem cells. *Stem Cell Rev Rep*. 2019;15(3):448–55. <https://doi.org/10.1007/s12015-019-09880-9>.
- D'Amato A, Mannelli LDC, Lucarini E, Man AL, Le Gall G, Branca JJV, et al. Faecal microbiota transplant from aged donor mice affects

- spatial learning and memory via modulating hippocampal synaptic plasticity- and neurotransmission-related proteins in young recipients. *Microbiome*. 2020;8(1). <https://doi.org/10.1186/s40168-020-00914-w>.
34. Deng L, Silins R, Castro-Mejía JL, Kot W, Jessen L, Thorsen J, et al. A protocol for extraction of infective viromes suitable for metagenomics sequencing from low volume fecal samples. *Viruses*. 2019;11(7). <https://doi.org/10.3390/v11070667>.
 35. Edwards AO, Ritter R, Abel KJ, Manning A, Panhuysen C, Farrer LA. Complement factor H polymorphism and age-related macular degeneration. *Science*. 2005;308(5720):421–4. <https://doi.org/10.1126/science.1110189>.
 36. Elderman M, Sovran B, Hugenholtz F, Graversen K, Huijskes M, Houtsma E, et al. The effect of age on the intestinal mucus thickness, microbiota composition and immunity in relation to sex in mice. *PLoS One*. 2017;12(9). <https://doi.org/10.1371/journal.pone.0184274>.
 37. Erny D, De Angelis ALH, Jaitin D, Wieghofer P, Staszewski O, David E, et al. Host microbiota constantly control maturation and function of microglia in the CNS. *Nat Neurosci*. 2015;18(7):965–77. <https://doi.org/10.1038/nn.4030>.
 38. Everard A, Belzer C, Geurts L, Ouwerkerk JP, Druart C, Bindels LB, et al. Cross-talk between *Akkermansia muciniphila* and intestinal epithelium controls diet-induced obesity. *Proc Natl Acad Sci U S A*. 2013;110(22):9066–71. <https://doi.org/10.1073/pnas.1219451110>.
 39. Franceschi C, Garagnani P, Parini P, Giuliani C, Santoro A. Inflammaging: a new immune–metabolic viewpoint for age-related diseases. *Nat Rev Endocrinol*. 2018. <https://doi.org/10.1038/s41574-018-0059-4> Nature Publishing Group.
 40. Fransen F, van Beek AA, Borghuis T, El Aidy S, Hugenholtz F, van der Gaast-de Jongh C, et al. Aged gut microbiota contributes to systemic inflammation after transfer to germ-free mice. *Front Immunol*. 2017;8(NOV):1385. <https://doi.org/10.3389/fimmu.2017.01385>.
 41. Franzosa EA, McIver LJ, Rahnavard G, Thompson LR, Schirmer M, Weingart G, et al. Species-level functional profiling of metagenomes and metatranscriptomes. *Nat Methods*. 2018;15(11):962–8. <https://doi.org/10.1038/s41592-018-0176-y>.
 42. Gajda AM, Storch J. Enterocyte fatty acid-binding proteins (FABPs): different functions of liver and intestinal FABPs in the intestine. *Prostaglandins Leukot Essent Fat Acids*. 2015;93(February):9–16. <https://doi.org/10.1016/j.plefa.2014.10.001>.
 43. Ghosh TS, Das M, Jeffery IB, O'Toole PW, O'Toole PW. Adjusting for age improves identification of gut microbiome alterations in multiple diseases. *ELife*. 2020;9(March). <https://doi.org/10.7554/eLife.50240>.
 44. Gloor GB, Wu JR, Pawlowsky-Glahn V, Egozcue JJ. It's all relative: analyzing microbiome data as compositions. *Ann Epidemiol*. 2016. <https://doi.org/10.1016/j.jannepidem.2016.03.003>.
 45. Ha JY, Choi S-Y, Lee JH, Hong S-H, Lee H-J. Delivery of periodontopathogenic extracellular vesicles to brain monocytes and microglial IL-6 promotion by RNA cargo. *Front Mol Biosci*. 2020;7(November). <https://doi.org/10.3389/fmols.2020.596366>.
 46. Hageman GS, Anderson DH, Johnson LV, Hancox LS, Taiber AJ, Hardisty LJ, et al. A common haplotype in the complement regulatory gene factor H (HF1/CFH) predisposes individuals to age-related macular degeneration. *Proc Natl Acad Sci U S A*. 2005;102(20):7227–32. <https://doi.org/10.1073/pnas.0501536102>.
 47. Han EC, Choi SY, Lee Y, Park JW, Hong SH, Lee HJ. Extracellular RNAs in periodontopathogenic outer membrane vesicles promote TNF- α production in human macrophages and cross the blood-brain barrier in mice. *FASEB J*. 2019;33(12):13412–22. <https://doi.org/10.1096/fj.201901575R>.
 48. Heneka MT. Microglia take Centre stage in neurodegenerative disease. *Nat Rev Immunol*. 2019;19(2):79–80. <https://doi.org/10.1038/s41577-018-0112-5>.
 49. Hopkins MJ, Sharp R, Macfarlane GT. Age and disease related changes in intestinal bacterial populations assessed by cell culture, 16S rRNA abundance, and community cellular fatty acid profiles. *Gut*. 2001;48(2):198–205. <https://doi.org/10.1136/gut.48.2.198>.
 50. Horai R, Zárate-Bladés CR, Dillenburg-Pilla P, Chen J, Kielczewski JL, Silver PB, et al. Microbiota-dependent activation of an autoreactive T cell receptor provokes autoimmunity in an immunologically privileged site. *Immunity*. 2015;43(2):343–53. <https://doi.org/10.1016/j.immuni.2015.07.014>.
 51. Hothorn T, Hornik K, Van De Wiel MA, Zeileis A. A lego system for conditional inference. *Am Stat*. 2006;60(3):257–63. <https://doi.org/10.1198/000313006X118430>.
 52. Iljazovic A, Roy U, Gálvez EJCC, Lesker TR, Zhao B, Gronow A, et al. Perturbation of the gut microbiome by *Prevotella* spp. enhances host susceptibility to mucosal inflammation. *Mucosal Immunol*. 2020;May:1–12. <https://doi.org/10.1038/s41385-020-0296-4>.
 53. James SA, et al. Preterm infants harbour a rapidly changing mycobiota that includes *Candida* pathobionts. *J Fungi*. 2020;no. jof-995977.
 54. Kabouridis PSS, Lasrado R, McCallum S, Chng SHH, Snippet HJJ, Clevers H, et al. Microbiota controls the homeostasis of glial cells in the gut lamina propria. *Neuron*. 2015;85(2):289–95. <https://doi.org/10.1016/j.NEURON.2014.12.037>.
 55. Kam JH, Lenassi E, Jeffery G. Viewing ageing eyes: diverse sites of amyloid beta accumulation in the ageing mouse retina and the up-regulation of macrophages. *PLoS One*. 2010;5(10). <https://doi.org/10.1371/journal.pone.0013127>.
 56. Kim KA, Jeong JJ, Yoo SY, Kim DH. Gut microbiota lipopolysaccharide accelerates inflamm-aging in mice. *BMC Microbiol*. 2016;16(1). <https://doi.org/10.1186/s12866-016-0625-7>.
 57. Kim MS, Kim Y, Choi HH, Kim W, Park S, Lee DS, et al. Transfer of a healthy microbiota reduces amyloid and tau pathology in an Alzheimer's disease animal model. *Gut*. 2020;69(2):283–94. <https://doi.org/10.1136/gutjnl-2018-317431>.
 58. Kim SM, McIlwraith EK, Chalmers JA, Belsham DD. Palmitate induces an anti-inflammatory response in immortalized microglial BV-2 and IMG cell lines that decreases TNF α levels in MHypoE-46 hypothalamic neurons in co-culture. *Neuroendocrinology*. 2018;107(4):387–99. <https://doi.org/10.1159/000494759>.
 59. Klein RJ, Zeiss C, Chew EY, Tsai JY, Sackler RS, Haynes C, et al. Complement factor H polymorphism in age-related macular degeneration. *Science*. 2005;308(5720):385–9. <https://doi.org/10.1126/science.1109557>.
 60. Kovatcheva-Datchary P, Nilsson A, Akrami R, Lee YS, De Vadder F, Arora T, et al. Dietary fiber-induced improvement in glucose metabolism is associated with increased abundance of *Prevotella*. *Cell Metab*. 2015;22(6):971–82. <https://doi.org/10.1016/j.cmet.2015.10.001>.
 61. Kundu P, Lee HU, Garcia-Perez I, Tay EXY, Kim H, Faylon LE, et al. Neurogenesis and longevity signaling in young germ-free mice transplanted with the gut microbiota of old mice. *Sci Transl Med*. 2019;11(518). <https://doi.org/10.1126/scitranslmed.aau4760>.
 62. Kutty RK, Samuel W, Abay R, Cherukuri A, Nagineni CN, Duncan T, et al. Resveratrol attenuates CXCL11 expression induced by proinflammatory cytokines in retinal pigment epithelial cells. *Cytokine*. 2015;74(2):335. <https://doi.org/10.1016/j.cyt.2015.03.016>.
 63. Lahti L, Sudarshan Shetty T, Blake, and J Salojärvi. Tools for microbiome analysis in R. microbiome package version. *Bioconductor*. 2019.
 64. Langille MG, Meehan CJ, Koenig JE, Dhanani AS, Rose RA, Howlett SE, et al. Microbial shifts in the aging mouse gut. *Microbiome*. 2014;2(1). <https://doi.org/10.1186/s40168-014-0050-9>.
 65. Langmann T. Microglia activation in retinal degeneration. *J Leukoc Biol*. 2007;81(6):1345–51. <https://doi.org/10.1189/jlb.0207114>.
 66. Lau E, Marques C, Pestana D, Santoalha M, Carvalho D, Freitas P, et al. The role of I-FABP as a biomarker of intestinal barrier dysfunction driven by gut microbiota changes in obesity. *Nutr Metab*. 2016;13(1). <https://doi.org/10.1186/s12986-016-0089-7>.
 67. LeGall G. NMR spectroscopy of biofluids and extracts. *Methods Mol Biol*. 2015;1277:29–36. https://doi.org/10.1007/978-1-4939-2377-9_3.
 68. LeGall G, Noor SO, Ridgway K, Scovell L, Jamieson C, Johnson IT, et al. Metabolomics of fecal extracts detects altered metabolic activity of gut microbiota in ulcerative colitis and irritable bowel syndrome. *J Proteome Res*. 2011;10(9):4208–18. <https://doi.org/10.1021/pr2003598>.
 69. Lenth, Rs. 2020. "Emmeans: estimated marginal means, aka least-squares means. R Package Version 1.4.5"
 70. Leyrolle Q, Layé S, Nadjar A. Direct and indirect effects of lipids on microglia function. *Neurosci Lett*. 2019. <https://doi.org/10.1016/j.neulet.2019.134348> Elsevier Ireland Ltd.
 71. Li Z, Sheng L. Significance of dynamic evolution of TNF- α , IL-6 and intestinal fatty acid-binding protein levels in neonatal necrotizing enterocolitis. *Exper Ther Med*. 2018;15(2):1289–92. <https://doi.org/10.3892/etm.2017.5532>.

72. Lin JB, Tsubota K, Apte RS. A glimpse at the aging eye. *Npj Aging Mech Dis.* 2016;2(1):1–7. <https://doi.org/10.1038/npjamd.2016.3>.
73. van der Lugt B, van Beek AA, Aalvink S, Meijer B, Sovran B, Vermeij WP, et al. Akkermansia muciniphila ameliorates the age-related decline in colonic mucus thickness and attenuates immune activation in accelerated aging Ercc1- Δ 7 mice. *Immun Ageing.* 2019;16:6. <https://doi.org/10.1186/s12979-019-0145-z>.
74. Ma J, Hong Y, Zheng N, Xie G, Yuanzhi Lyu YG, Xi C, et al. Gut microbiota remodeling reverses aging-associated inflammation and dysregulation of systemic bile acid homeostasis in mice sex-specifically. *Gut Microbes.* 2020;11(5):1450–74. <https://doi.org/10.1080/19490976.2020.1763770>.
75. Ma TY, Hollander D, Dadufalza V, Krugliak P. Effect of aging and caloric restriction on intestinal permeability. *Exp Gerontol.* 1992;27(3):321–33. [https://doi.org/10.1016/0531-5565\(92\)90059-9](https://doi.org/10.1016/0531-5565(92)90059-9).
76. Mabbott NA, Kobayashi A, Sehgal A, Bradford BM, Pattison M, Donaldson DS. Aging and the mucosal immune system in the intestine. In: *Biogerontology*: Kluwer Academic Publishers; 2015. <https://doi.org/10.1007/s10522-014-9498-z>.
77. Mahnert A, Blohs M, Pausan MR, Moissl-Eichinger C. The human archaeome: methodological pitfalls and knowledge gaps. In: *Emerging topics in life sciences*: Portland Press Ltd.; 2018. <https://doi.org/10.1042/ETLS20180037>.
78. Matsumoto M, Kurihara S, Kibe R, Ashida H, Benno Y. Longevity in mice is promoted by probiotic-induced suppression of colonic senescence dependent on upregulation of gut bacterial polyamine production. *PLoS One.* 2011;6(8). <https://doi.org/10.1371/journal.pone.0023652>.
79. McMurdie PJ, Holmes S. Phyloseq: an R package for reproducible interactive analysis and graphics of microbiome census data. Edited by Michael Watson. *PLoS ONE.* 2013;8(4):e61217. <https://doi.org/10.1371/journal.pone.0061217>.
80. Melo HM, Gisele da S, da Silva S, Ramos M, Sant'Ana CVLT, Clarke JR, et al. Palmitate is increased in the cerebrospinal fluid of humans with obesity and induces memory impairment in mice via pro-inflammatory TNF- α . *Cell Rep.* 2020;30(7):2180–2194.e8. <https://doi.org/10.1016/j.celrep.2020.01.072>.
81. Million M, Angelakis E, Maraninchi M, Henry M, Giorgi R, Valero R, et al. Correlation between body mass index and gut concentrations of lactobacillus reuteri, Bifidobacterium animalis, Methanobrevibacter smithii and Escherichia coli. *Int J Obes.* 2013;37(11):1460–6. <https://doi.org/10.1038/ijo.2013.20>.
82. Mosher KI, Wyss-Coray T. Microglial dysfunction in brain aging and Alzheimer's disease. *Biochem Pharmacol.* 2014. <https://doi.org/10.1016/j.bcp.2014.01.008>.
83. Nalapareddy K, Nattamai KJ, Kumar RS, Karns R, Wikenheiser-Brookamp KA, Sampson LL, et al. Canonical Wnt signaling ameliorates aging of intestinal stem cells. *Cell Rep.* 2017;18(11):2608–21. <https://doi.org/10.1016/j.celrep.2017.02.056>.
84. Natoli R, Fernando N, Madigan M, Chu-Tan JA, Valter K, Provis J, et al. Microglia-derived IL-1 β promotes chemokine expression by Müller cells and RPE in focal retinal degeneration. *Mol Neurodegener.* 2017;12(1). <https://doi.org/10.1186/S13024-017-0175-Y>.
85. Nicoletti C. Age-associated changes of the intestinal epithelial barrier: local and systemic implications. 2015;9(12):1467–9. <https://doi.org/10.1586/17474124.2015.1092872>.
86. O'Toole PW, Jeffery IB. Gut microbiota and aging: Science. American Association for the Advancement of Science; 2015. <https://doi.org/10.1126/science.aac8469>.
87. Odamaki T, Kato K, Sugahara H, Hashikura N, Takahashi S, Xiao JZ, et al. Age-related changes in gut microbiota composition from newborn to centenarian: a cross-sectional study. *BMC Microbiol.* 2016;16(1):90. <https://doi.org/10.1186/s12866-016-0708-5>.
88. Ohno-Matsui K. Parallel findings in age-related macular degeneration and Alzheimer's disease. In: *Progress in retinal and eye research*: Pergamon; 2011. <https://doi.org/10.1016/j.preteyeres.2011.02.004>.
89. Oksanen J, Blanchet FG, Friendly M, Kindt R, Legendre P, Mcglinn D, et al. Package 'vegan' title community ecology package version 2.5-7; 2020.
90. Parker A, Fonseca S, Carding SR. Gut microbes and metabolites as modulators of blood-brain barrier integrity and brain health: Taylor and Francis Inc.; 2020. <https://doi.org/10.1080/19490976.2019.1638722>. *Gut Microbes*
91. Pontifex MG, Martinsen A, Rasha NM, Saleh GH, Tejera N, Müller M, et al. APOE4 genotype exacerbates the impact of menopause on cognition and synaptic plasticity in APOE-TR mice. *FASEB J.* 2021;35(5):e21583. <https://doi.org/10.1096/FJ.202002621RR>.
92. R Core Team. R: a language and environment for statistical computing. Vienna: Foundation for Statistical Computing; 2013. <http://www.r-project.org/>
93. Leung R, Proitsi P, Simmons A, Lunnon K, Güntert A, Kronenberg D, et al. Inflammatory proteins in plasma are associated with severity of Alzheimer's disease. *PLoS One.* 2013;8(6). <https://doi.org/10.1371/JOURNAL.PONE.0064971>.
94. Ramos-Molina B, Queipo-Ortuño MI, Lambertos A, Tinahones FJ, Peñafiel R. Dietary and gut microbiota polyamines in obesity- and age-related diseases. *Front Nutr.* 2019. <https://doi.org/10.3389/fnut.2019.00024>.
95. Rea IM, Gibson DS, McGilligan V, McNerlan SE, Denis Alexander H, Ross OA. Age and age-related diseases: role of inflammation triggers and cytokines. *Front Immunol.* 2018. <https://doi.org/10.3389/fimmu.2018.00586>.
96. Rohart F, Gautier B, Singh A, Cao K-AL. "MixOmics: an R package for 'omics feature selection and multiple data integration." edited by Dina Schneidman. *PLoS Comput Biol.* 2017;13(11):e1005752. <https://doi.org/10.1371/journal.pcbi.1005752>.
97. Romano S, Savva GM, Bedarf JR, Charles IG, Hildebrand F, Narbad A. Meta-analysis of the gut microbiome of Parkinson's disease patients suggests alterations linked to intestinal inflammation. *MedRxiv.* 2020;2020(08):10.20171397. <https://doi.org/10.1101/2020.08.10.20171397>.
98. Rossi S, Mancino R, Bergami A, Mori F, Castellì M, De Chiara V, et al. Potential role of IL-13 in neuroprotection and cortical excitability regulation in multiple sclerosis. 2011;17(11):1301–12. <https://doi.org/10.1177/1352458511410342>.
99. Rowan S, Jiang S, Korem T, Szymanski J, Chang M-LL, Szegöl J, et al. Involvement of a gut-retina axis in protection against dietary glycaemia-induced age-related macular degeneration. *Proc Natl Acad Sci U S A.* 2017;114(22):E4472–81. <https://doi.org/10.1073/pnas.1702302114>.
100. Rowan S, Taylor A. The role of microbiota in retinal disease. *Adv Exp Med Biol.* 2018;1074:429–35. https://doi.org/10.1007/978-3-319-75402-4_53.
101. Rueden CT, Schindelin J, Hiner MC, DeZonia BE, Walter AE, Arena ET, et al. ImageJ2: ImageJ for the next generation of scientific image data. *BMC Bioinformatics.* 2017;18(1):529. <https://doi.org/10.1186/s12859-017-1934-z>.
102. Rutar, Matt, Riccardo Natoli, RX Chia, Krisztina Valter, and Jan M Provis. 2015. "Chemokine-mediated inflammation in the degenerating retina is coordinated by Müller cells, activated microglia, and retinal pigment epithelium." *J Neuroinflammation* 12 (1): 1–15. <https://doi.org/10.1186/S12974-014-0224-1>.
103. Rutar M, Valter K, Natoli R, Provis JM. "Synthesis and propagation of complement C3 by microglia/monocytes in the aging retina." edited by Erica Lucy fletcher. *PLoS One.* 2014;9(4):e93343. <https://doi.org/10.1371/journal.pone.0093343>.
104. Scher JU, Sczesnak A, Longman RS, Segata N, Ubeda C, Bielski C, et al. Expansion of intestinal Prevotella copri correlates with enhanced susceptibility to arthritis. *ELife.* 2013;2(12):1202. <https://doi.org/10.7554/eLife.01202.001>.
105. Schindelin J, Arganda-Carreras I, Frise E, Kaynig V, Longair M, Pietzsch T, et al. Fiji: an open-source platform for biological-image analysis. *Nat Methods.* 2012. <https://doi.org/10.1038/nmeth.2019> Nature Publishing Group.
106. Scott KA, Ida M, Peterson VL, Prenderville JA, Moloney GM, Izumo T, et al. Revisiting Metchnikoff: age-related alterations in microbiota-gut-brain axis in the mouse. *Brain Behav Immun.* 2017;65(October):20–32. <https://doi.org/10.1016/j.bbi.2017.02.004>.
107. Segata N, Waldron L, Ballarini A, Narasimhan V, Jousson O, Huttenhower C. Metagenomic microbial community profiling using unique clade-specific marker genes. *Nat Methods.* 2012;9(8):811–4. <https://doi.org/10.1038/nmeth.2066>.
108. Shinham H, Hogg C, Jeffery G. Long wavelength light that improves aged mitochondrial function selectively increases cytokine expression

- in serum and the retina. *BioRxiv*. 2021:10.468030. <https://doi.org/10.1101/2021.11.10.468030>.
109. Sierra A, Gottfried-Blackmore AC, McEwen BS, Bulloch K. Microglia derived from aging mice exhibit an altered inflammatory profile. *Glia*. 2007;55(4):412–24. <https://doi.org/10.1002/glia.20468>.
 110. Smith P, Willemsen D, Popkes M, Metge F, Gandiwa E, Reichard M, et al. Regulation of life span by the gut microbiota in the short-lived African turquoise killifish. *eLife*. 2017;6(August). <https://doi.org/10.7554/eLife.27014>.
 111. Sommer F, Bäckhed F. The gut microbiota-masters of host development and physiology. *Nat Rev Microbiol*. 2013. <https://doi.org/10.1038/nrmicro.2974>.
 112. Stebbegg M, Silva-Cayetano A, Innocenti S, Jenkins TP, Cantacessi C, Gilbert C, et al. Heterochronic faecal transplantation boosts gut germinal centres in aged mice. *Nat Commun*. 2019;10(1). <https://doi.org/10.1038/s41467-019-10430-7>.
 113. Su T, Liu R, Lee A, Long Y, Lijun D, Lai S, et al. Altered intestinal microbiota with increased abundance of *Prevotella* is associated with high risk of diarrhea-predominant irritable bowel syndrome. *Gastroenterol Res Pract*. 2018;2018. <https://doi.org/10.1155/2018/6961783>.
 114. Sugano E, Tabata K, Takezawa T, Shiraiwa R, Muraoka H, Metoki T, et al. N-methyl-N-nitrosourea-induced photoreceptor degeneration is inhibited by nicotinamide via the blockade of upstream events before the phosphorylation of signalling proteins. *Biomed Res Int*. 2019;2019. <https://doi.org/10.1155/2019/3238719>.
 115. Sun J, Jingxuan X, Ling Y, Wang F, Gong T, Yang C, et al. Fecal microbiota transplantation alleviated Alzheimer's disease-like pathogenesis in APP/PS1 transgenic mice. *Transl Psychiatry*. 2019;9(1):1–13. <https://doi.org/10.1038/s41398-019-0525-3>.
 116. Suzek BE, Wang Y, Huang H, McGarvey PB, Cathy HW. UniRef clusters: a comprehensive and scalable alternative for improving sequence similarity searches. *Bioinformatics*. 2015;31(6):926–32. <https://doi.org/10.1093/bioinformatics/btu739>.
 117. "The Jamovi Project (2020). Jamovi (Version 1.2) [Computer Software]."
 118. Thevaranjan N, Puchta A, Schulz C, Avee Naidoo JC, Szamosi CP, Verschoor DL, et al. Age-associated microbial dysbiosis promotes intestinal permeability, systemic inflammation, and macrophage dysfunction. *Cell Host Microbe*. 2017;21(4):455–466.e4. <https://doi.org/10.1016/j.chom.2017.03.002>.
 119. Tracy LM, Bergqvist F, Ivanova EV, Jacobsen KT, Iverfeldt K. Exposure to the saturated free fatty acid palmitate alters BV-2 microglia inflammatory response. *J Mol Neurosci*. 2013;51(3):805–12. <https://doi.org/10.1007/s12031-013-0068-7>.
 120. Tran L, Meerveld BG-V. Age-associated remodeling of the intestinal epithelial barrier. *J Gerontol- Ser A Biol Sci Med Sci*. 2013;68(9):1045–56. <https://doi.org/10.1093/gerona/glt106>.
 121. Tran TTTT, Corsini S, Kellingray L, Hegarty C, Le Gall G, Narbad A, et al. APOE genotype influences the gut microbiome structure and function in humans and mice: relevance for Alzheimer's disease pathophysiology. *FASEB J*. 2019;33(7):8221–31. <https://doi.org/10.1096/fj.20190071R>.
 122. Valenzano DR, Seidel J. The role of the gut microbiome during host ageing [version 1; referees: 2 approved]. *F1000Research*. 2018. <https://doi.org/10.12688/f1000research.15121.1>.
 123. Villeda LJ, Mosher KI, Zou B, Britschgi M, Bieri G, Stan TM, et al. The ageing systemic milieu negatively regulates neurogenesis and cognitive function. *Nature*. 2011;477(7362):90–6. <https://doi.org/10.1038/nature10357>.
 124. Wei S, Peng W, Mai Y, Li K, Wei W, Li H, et al. Outer membrane vesicles enhance tau phosphorylation and contribute to cognitive impairment. *J Cell Physiol*. 2020;235(5):4843–55. <https://doi.org/10.1002/jcp.29362>.
 125. Wells JM, Brummer RJ, Derrien M, MacDonald TT, Troost F, Cani PD, et al. Homeostasis of the gut barrier and potential biomarkers. *Am J Physiol Gastrointest Liver Physiol*. 2017. <https://doi.org/10.1152/ajpgi.00048.2015>.
 126. Wells PM, Adebayo AS, Bowyer RCE, Freidin MB, Finckh A, Strowig T, et al. Associations between gut microbiota and genetic risk for rheumatoid arthritis in the absence of disease: a cross-sectional study. *Lancet Rheumatol*. 2020;2(7):e418–27. [https://doi.org/10.1016/S2665-9913\(20\)30064-3](https://doi.org/10.1016/S2665-9913(20)30064-3).
 127. Wiercinska-Drapalo A, Jaroszewicz J, Siwak E, Pogorzelska J, Prokopowicz D. Intestinal fatty acid binding protein (I-FABP) as a possible biomarker of ileitis in patients with ulcerative colitis. *Regul Pept*. 2008;147(1–3):25–8. <https://doi.org/10.1016/j.regpep.2007.12.002>.
 128. Winter SE, Bäuml AJ. Dysbiosis in the inflamed intestine. *Gut Microbes*. 2014;5(1):71–3. <https://doi.org/10.4161/gmic.27129>.
 129. Xu H, Chen M, Forrester JV. Para-inflammation in the aging retina. In: *Progress in Retinal and Eye Research*: Pergamon; 2009. <https://doi.org/10.1016/j.preteyeres.2009.06.001>.
 130. Zhao BY, Xie W, Shi X, Li F, Yang F, Sun Y, et al. Interleukin-1 β level is increased in vitreous of patients with neovascular age-related macular degeneration (NAMD) and polypoidal choroidal vasculopathy (PCV). *PLoS One*. 2015;10(5). <https://doi.org/10.1371/JOURNAL.PONE.0125150>.
 131. Zinkernagel MS, Zysset-Burri DC, Keller I, Berger LE, Leichtle AB, Largiadèr CR, et al. Association of the intestinal microbiome with the development of neovascular age-related macular degeneration. *Sci Rep*. 2017;7(1):1–9. <https://doi.org/10.1038/srep40826>.
 132. Zuo T, Ng S C. The gut microbiota in the pathogenesis and therapeutics of inflammatory bowel disease. *Front Microbiol*. 2018. <https://doi.org/10.3389/fmicb.2018.02247>.
 133. Zysset-Burri DC, Keller I, Berger LE, Largiadèr CR, Wittwer M, Wolf S, et al. Associations of the intestinal microbiome with the complement system in neovascular age-related macular degeneration. *Npj Genom Med*. 2020;5(1):34. <https://doi.org/10.1038/s41525-020-00141-0>.

Publisher's Note

Springer Nature remains neutral with regard to jurisdictional claims in published maps and institutional affiliations.

Ready to submit your research? Choose BMC and benefit from:

- fast, convenient online submission
- thorough peer review by experienced researchers in your field
- rapid publication on acceptance
- support for research data, including large and complex data types
- gold Open Access which fosters wider collaboration and increased citations
- maximum visibility for your research: over 100M website views per year

At BMC, research is always in progress.

Learn more biomedcentral.com/submissions

